

## Photon Diffractive Dissociation in Deep Inelastic Scattering

**E. Levin**<sup>1</sup>

*Fermilab, P.O. Box 500, Batavia, Il 60510, USA*

and

**M. Wüsthoff**

*II. Institut für Theoretische Physik, Universität Hamburg, Germany*

### Abstract

This paper is mainly devoted to the presentation and discussion of formulas for the cross section of photon diffractive dissociation. The calculations which we present in a very detailed way are based on perturbative QCD. We improve formulas which describe this process in the Triple Regge Limit where the square of the missing mass  $M_X$  (the invariant mass of the bunch of secondary hadrons) is much larger than  $|Q^2|$  and extend the range of validity to the region where  $M_X^2$  is of the same order as  $|Q^2|$ . The comparison with calculations done by Mueller and Qui [1] leads us to the conclusion that whenever quarks are involved in the triple ladder vertex the AGK cutting rules are violated whereas for gluons these rules seem to work.

---

<sup>1</sup>On leave from St.Petersbourg Nuclear Physics Institute, 188350 Gatchina, Russia



# 1 Introduction:

Diffraction dissociation processes in general provides us with the basic information on the dynamics of "soft" interaction. In the framework of the old-fashioned reggeon approach the soft interaction at high energies was reduced to the interaction between Pomerons via the triple Pomeron coupling constant ( $G_{3P}$  see fig. 1.1). Its value was extracted from experimental data on diffractive dissociation with a large missing mass (invariant mass of the bunch of secondary hadrons  $M_X$ ) [?, ?] (see fig. 1.1). Although there are large uncertainties in the value of  $G_{3P}$  (see [?]) the process of diffractive dissociation gives the only possibility to estimate this value.

The process of diffractive dissociation in deep inelastic scattering looks especially interesting for three reasons:

1. The natural scale of hardness, namely, the large value of  $|Q^2|$  (see fig. 1.2) gives hope to develop the theoretical approach to this process within perturbative QCD. Such an approach was suggested in the paper of GLR [?] and has been developed in a series of recent papers [?, ?, ?].

2. The virtual photon in the diffractive dissociation probes the structure of the Pomeron. This means that this process could lead to a better understanding of the Pomeron structure. The idea to describe the diffractive dissociation process with the help of a Pomeron structure function was firstly introduced by Ingelman and Schlein [?] and has been discussed from another point of view in ref. [?, ?, ?, ?]. The perturbative approach to the diffractive dissociation allows to examine the above ideas on a theoretical basis and helps to clarify what the Pomeron structure is.

3. The diffractive dissociation in deep inelastic scattering is closely related to the screening (shadowing) corrections in deep inelastic scattering through the AGK cutting rules [?] as was noted in [?]. So diffractive dissociation can give direct information on the screening (shadowing) corrections, and the theoretical understanding of their nature is equivalent to the understanding of the nature of the screening (shadowing) corrections. Moreover, experimental studies of diffractive dissociation will test our understanding of screening corrections in the most direct way.

The main goal of this paper is to develop the Leading Log Approximation (LLA) of the diffractive dissociation of the virtual photon in the framework of perturbative QCD and to present reliable formulas for this process. We should mention that we cannot present the final answer of this process but we hope that this paper is the first stage of the theoretical approach and provides a solid basis for the interpretation of HERA's future experimental data.

The paper is organized in the following way: in section 2 we discuss the kinematics, the

small parameters and the main results which include the evolution equation of the process and some comparison of the idea of the Pomeron structure function with our QCD approach. Section 3 contains the Born approximation of the production of two quarks, i.e. quark and anti-quark, and the production of two quarks with an additional gluon (3-jet event). Section 4 deals with the problem how to generalize to an infinite number of jets. In section 5 we summarize our results, and the appendix contains all technical details of the calculations.

## 2 The strategy of the approach and the main results:

### 2.1 Kinematics and notations:

In this section we would like to outline our approach and we begin with the kinematics and the notations that we are going to use throughout the paper.

First of all we would like to introduce the light-cone vector  $Q'_\mu$  which characterizes the incoming virtual photon.

$$Q'_\mu = Q_\mu + x_B p_\mu \quad (2.1)$$

where

$$x_B = \frac{|Q^2|}{2(Q, p)} \quad (2.2)$$

is the usual Bjorken variable. The main property of  $Q'_\mu$  is the fact that

$$Q'^2 = Q^2 + 2x_B(Q, p) = 0 \quad (2.3)$$

As energy variable we use

$$s = 2(Q, p) \quad (2.4)$$

It is easy to see that

$$\bar{s} \equiv (Q + p)^2 = (1 - x_B)s \quad (2.5)$$

We expand all the momenta of the particles in our reaction in terms of  $Q'_\mu$  and  $p_\mu$  using Sudakov variables [?]. As example we take the momentum  $u$  OBwhich is transferred along the Pomeron and write it as:

$$u_\mu = \alpha_u Q'_\mu + \beta_u p_\mu + u_{t\mu} \quad (2.6)$$

Using eq. (2.6) we can express the mass of the produced particles  $M_X^2$  through  $\alpha_u$  and  $\beta_u$  in the following way:

$$M_X^2 = (Q + u)^2 = (1 + \alpha_u)(\beta_u - x_B)s + u_t^2 \quad (2.7)$$

while

$$(p - u)^2 = m^2 \quad \text{or} \quad \alpha_u s - u_t^2 \approx 0 \quad (2.8)$$

From eq. (2.7) and (2.8) we get

$$\begin{aligned} \beta_u &= \frac{M_X^2 + x_B s - u_t^2}{(1 + \alpha_u)s} \\ &\approx \frac{M_X^2 + x_B s - u_t^2}{s} \\ &\approx \frac{M_X^2 + |Q^2|}{s} \end{aligned} \quad (2.9)$$

since  $|\alpha_u| = \frac{u_t^2}{s} \ll 1$ .

An important assumption for the diffractive dissociation process is the smallness of the missing mass  $M_X$  compared to the total energy  $\sqrt{s} \approx \sqrt{s}$ . This means that (see eq. (2.9))

$$\beta_u - x_B \ll 1 \quad (2.10)$$

For each produced particle we have the condition that its energy is positive. With this condition we can formulate the following constraints on  $\alpha_i$  and  $\beta_i$ :

$$\begin{aligned} \alpha_i Q_0 + (\beta_i + \alpha_i x_B) p_0 &> 0 \\ -\alpha_u Q_0 + (1 - \beta_u - \alpha_u x_B) p_0 &> 0 \end{aligned} \quad (2.11)$$

Finally, the energy momentum conservation leads to the equation:

$$\begin{aligned} 1 + \alpha_u &= \sum_i \alpha_i \\ \beta_u + x_B &= \sum_i \beta_i \end{aligned} \quad (2.12)$$

## 2.2 The scale of hardness:

If we want to apply perturbative QCD to the diffractive dissociation process, we need to specify the scale of hardness that appears in this process. Our first and natural scale is the large value of  $|Q^2|$ . But, this scale is not enough to apply the method of perturbative QCD. We need to specify what the Pomeron in QCD is. Our present understanding of the Pomeron in QCD could be expressed in the following way: the Pomeron is a ladder diagram (see fig. 2.1). This approach can be justified only, if we assume that the initial virtuality  $|Q_0^2|$  is sufficiently large and the final virtuality  $|\bar{Q}_0^2|$  lies far above the initial one, namely,

$$|\bar{Q}_0^2| \gg |Q_0^2| \quad \text{and} \quad \alpha_s(|Q_0^2|) \ll 1 \quad (2.13)$$

It has to be stressed that we have to introduce both parameters  $Q_0$  and  $\bar{Q}_0$  ad hoc. Indeed,  $|Q_0^2|$  (transverse momentum of the parton inside the proton) is the starting value for the GLAP-evolution equation [?]. If we know the proton structure function at  $|Q_0^2|$ , the GLAP-evolution equation gives the structure function at the larger scale  $|Q^2|$ . However, in the diffractive dissociation only partons with a transverse momentum which is substantially smaller than  $|Q^2|$  are involved. In order to treat this case we need to assume that the minimal transverse momentum of the produced particles is large enough ( $|k_{i_t}| \geq |\bar{Q}_0|$ ) to be sure that perturbative QCD still works while calculating the cross section. A negative consequence is that we cannot calculate the total cross section of diffractive dissociation. What we actually do is to calculate a part of the diffractive dissociation, namely, the cross section of the following process:

$$\gamma^*(Q^2) + p \rightarrow \text{jets}(|k_{i_{\text{jet}}}| \geq |\bar{Q}_0|) + X + p' \quad (2.14)$$

Now, we would like to summarize what we are able to calculate. It is the process of jet production in the diffractive dissociation with

$$|k_{i_{\text{jet}}}| \geq |\bar{Q}_0| \quad \text{where} \quad |Q^2| \gg |\bar{Q}_0^2| \gg |Q_0^2| \quad (2.15)$$

In the course of our paper we will discuss the natural scale for  $|\bar{Q}_0^2|$ , and we will present some estimates for the total cross section of diffractive dissociation.

### 2.3 Small parameters and leading logs of the approach:

In this subsection we would like to clarify what our small parameters are and which type of logs we are able to sum in the Leading Log Approximation (LLA) of perturbative QCD. We first have a look on the Double Leading log Approximation (DLA). This approximation was used in earlier calculations of diffractive dissociation [?, ?]. It is capable to explain the most typical and important features of this process. In our paper we concentrate on the generalization to the case of single leading log approximation and do some improvement in the DLA-region.

Now let us list the parameters for DLA:

$$\begin{aligned} \alpha_s \ln \frac{\beta_u}{x_B} \leq 1 \quad , \quad \alpha_s \ln \frac{Q^2}{\bar{Q}_0^2} \leq 1 \\ \alpha_s (|\bar{Q}_0^2|) \ll 1 \\ \alpha_s \ln \frac{\beta_u}{x_B} \ln \frac{Q^2}{\bar{Q}_0^2} \geq 1 \end{aligned} \quad (2.16)$$

and

$$\begin{aligned}
\alpha_s \ln \frac{1}{\beta_u} \leq 1 \quad , \quad \alpha_s \ln \frac{\bar{Q}_0^2}{Q_0^2} \leq 1 \\
\alpha_s (|Q_0^2|) \ll 1 \\
\alpha_s \ln \frac{1}{\beta_u} \ln \frac{\bar{Q}_0^2}{Q_0^2} \geq 1 \quad .
\end{aligned}
\tag{2.17}$$

Using these small parameters we are able to calculate the cross section of the process shown in eq. (2.14) in the kinematical region:

$$\begin{aligned}
1 \gg \beta_u \gg x_B \\
|Q^2| \gg |\bar{Q}_0^2| \gg |Q_0^2| \\
|u_i^2| \ll |Q_0^2|
\end{aligned}
\tag{2.18}$$

The set of parameters in eq. (2.16) and (2.17) indicates the kind of logs we take into account. It is clear from fig. (2.2) that we sum all logs due to integration over  $\beta_i$  and  $k_{i_t}$  of the emitted partons ( $\ln \frac{1}{\beta_i} \ln |k_{i_t}^2|$ ) while we calculate the structure of the Pomeron in DLA.

The most important property of the cross section for diffractive dissociation in comparison to the usual leading log approach of the deep inelastic structure function is the higher twist integral over the transverse momentum of the slowest parton which has no logarithmic character and looks as follows (see also fig. 2.2):

$$\int_{|\bar{Q}_0^2|}^{|Q^2|} \frac{d|k_t^2|}{k_t^4}
\tag{2.19}$$

This integral indicates the need of introducing the lower cut off  $|\bar{Q}_0^2|$  for  $|k_t^2|$ . If there were none, the integral above could dominate at the absolutely lowest bound  $|Q_0^2|$ , i.e. there would be no room for the Pomeron to evolve. We have to take care and introduce a new lower bound which lies sufficiently far above  $|Q_0^2|$ . Another point which is illustrated by expression (2.19) is the fact that, since QCD is a dimensionless theory, the extra dimension coming from the integration over the momentum transferred along the Pomeron (in our case the integral over  $u_i^2$ ) is compensated by  $\frac{1}{|k_t^2|}$ . The extra power in the denominator of expression (2.19) also suggests the conclusion that the main contribution to the total cross section of reaction (2.14) originates from the region where  $k_t \approx \bar{Q}_0$  and that we can neglect logs of the type  $\ln \frac{k_t^2}{Q_0^2}$ . But this is not always the case <sup>2</sup>. As soon as we write down the corresponding evolution equation this problem becomes relevant, for we need to take the derivative of (2.19) at  $|Q^2|$  and all possible logs of the type  $\ln \frac{k_t^2}{Q_0^2}$  change into logs of the type  $\ln \frac{Q^2}{Q_0^2}$  which are essential.

---

<sup>2</sup>The complete integral over  $|k_t^2|$  could have a saddle point above  $|\bar{Q}_0^2|$ .

We are going to improve our DLA approach by expanding it to the following kinematical region:

$$\begin{aligned} 1 &\gg \beta_u \geq x_B \\ |Q^2| &\gg |\overline{Q}_0^2| \gg |Q_0^2| \\ |u_i^2| &\ll |Q_0^2| \end{aligned} \quad (2.20)$$

In this region we sum all logs  $\ln \frac{Q^2}{Q_0^2}$  but  $\alpha_s \ln \frac{x_B}{\beta_u} \ll 1$ . This means that the energy ( $\beta_i$  in fig. 1.2) of the produced particles may be uniformly distributed among them without any ordering. In this region it becomes very difficult to calculate all essential logs. In DLA we can manage this problem, but in the single log region  $\ln \frac{Q^2}{Q_0^2}$  we will neglect logs of the type  $\ln \frac{k^2}{Q_0^2}$  under the integral in (2.19). So, we face the problem now, that due to the complexity of the complete procedure we cannot do more than calculating the cross section in the kinematical region where the slowest produced jet has a transverse momentum close to  $\overline{Q}_0$ . But, we hope that a numerical analysis of this process will justify this restriction. More details about this problem will be given later.

There is one more kinematical region which may be studied with the help of the calculations presented in this paper<sup>3</sup>. This region is:

$$\begin{aligned} 1 &\gg \beta_u \gg x_B \\ |Q^2| &\geq |\overline{Q}_0^2| \gg |Q_0^2| \gg |u_i^2| \end{aligned} \quad (2.21)$$

In this case we have  $\alpha_s \ln \frac{\beta_u}{x_B} \geq 1$  but  $\alpha_s \ln \frac{Q^2}{Q_0^2} \ll 1$  and there is no ordering of the transverse momenta of the produced particles.

In the following we discuss two more regions which may be of interest for future experiments at HERA or hadron-hadron colliders which we have not calculated yet. The first region is:

$$\begin{aligned} 1 &\gg \beta_u \gg x_B \\ |Q^2| &\geq |u_i^2| \approx |\overline{Q}_0^2| \geq |Q_0^2| \end{aligned} \quad (2.22)$$

The momentum transferred along the Pomeron ( $u_i^2$ ) now plays the role of the lower cut off. This region is most natural for perturbative calculations since the Pomeron is now completely hard.

The second region is:

$$\begin{aligned} 1 &\gg \beta_u \gg x_B \\ |\overline{Q}_0^2| &\gg |Q^2| \gg |Q_0^2| \end{aligned} \quad (2.23)$$

---

<sup>3</sup>We do not consider this case explicitly.

In this kinematical region the jet production is the hard process and the jet with its large transverse momentum can be viewed as the probe of the process. The diffractive dissociation in deep inelastic scattering in this region is a good model for hard jet production in hadron-hadron collision.

At the end of this subsection we would like to mention another small parameter which is  $\frac{1}{N^4}$  where  $N$  denotes the number of colours. Due to this small parameter a large amount of gluon emission producing double logs of the type  $\ln \frac{\beta_u}{x_B} \ln \frac{k_t^2}{Q_0^2}$  is suppressed. This class of contributions we will neglect.

## 2.4 The main properties of the answer:

In this subsection we start the discussion of the final result for the cross section of reaction (2.14). The details of the calculation will be given in the next subsections.

The result is the generalized formula of GLR [?] now valid in the kinematical region (2.20) <sup>4</sup> and looks as follows <sup>5</sup>:

$$\begin{aligned}
& \frac{\beta_u d\sigma^{DD}}{d\beta_u d|u_t^2|} \left( \gamma^* + p \rightarrow jet(|k_t| > |\overline{Q}_0|) + X + p' \right) \Big|_{|u_t^2| \ll |Q_0^2|} = \\
& = \left| G_p^{2G}(|u_t^2|) \right|^2 \sum_F \frac{4\pi^2 e_F^2 \alpha_{em}}{|Q^2|} \int_{\frac{x}{\beta_u}}^1 \frac{dz}{z} \frac{x}{\beta_u} \int_{\frac{|\overline{Q}_0^2|}{1-z}}^{|Q^2|} \frac{d|k^2|}{k^4} \frac{\alpha_s((1-z)|k^2|)}{16} \cdot \\
& \cdot \left[ \Phi_P^F(z) D_F^F \left( \frac{x}{\beta_u z}, |Q^2|, |k^2| \right) + \Phi_P^G(z) D_G^F \left( \frac{x}{\beta_u z}, |Q^2|, |k^2| \right) + \right. \\
& + \frac{8N^2}{N^2 - 1} \frac{|k^2|}{z} \int_{\frac{x}{\beta_u z}}^1 \frac{dz'}{z'} \int_{\frac{|k^2|}{1-z'}}^{|Q^2|} \frac{d|q^2|}{q^4} \frac{\alpha_s((1-z')|q^2|)}{4\pi} \Phi_G^F(z') D_F^F \left( \frac{x}{\beta_u z z'}, |Q^2|, |q^2| \right) \Big] \cdot \\
& \cdot \left[ \beta_u D_P^G(\beta_u, |k^2|, |Q_0^2|) \right]^2 .
\end{aligned} \tag{2.24}$$

All notations should be clear from fig. 2.2.  $G_p^{2G}$  denotes the proton form factor which is 1 for  $u_t^2 = 0$ . Any function D stands for the particle distribution of a dressed parton (quark or gluon) after evolution from some low to some large virtuality. In expression (2.24) we have to be more careful with the treatment of our scales than we did before. As usual  $|Q^2|$  gives the upper bound of our virtualities  $|k^2|$  and  $|q^2|$ , but  $|\overline{Q}_0^2|$  we introduced as lower boundary of the transverse momentum squared  $|k_t^2|$ . Since we use  $|k^2|$  as variable of integration we have to divide  $\overline{Q}_0^2$  by  $1-z$  due to the relation  $|k_t^2| = (1-z)|k^2|$ . Which value the argument of  $\alpha_s$  should take can be found in ref. [?]. Following this paper we rescale the argument of  $\alpha_s$ ,

<sup>4</sup>except the third term in expr. (2.24) as will be explained under point 2 of this subsection

<sup>5</sup>for transverse polarized photons

from  $|k^2|$  to  $(1-z)|k^2|$ , i.e we take  $|k_t^2|$  as argument for  $\alpha_s$ . The main new results of equation (2.24) are the splitting functions  $\Phi_P^F$ ,  $\Phi_P^G$  and  $\bar{\Phi}_G^F$ . The first two describe the interaction of the Pomeron with quarks and gluons. New in comparison with the GLR-formula is the Pomeron interaction with quarks. This process has been calculated in the paper [?] and [?] but with two different results. So we repeated the calculation in a slightly different technique and found the splitting function  $\Phi_P^F$  which is the corrected version of [?] and which coincides with the result in [?]. Besides, we found the second splitting function  $\Phi_P^G$  which describes the interaction of the Pomeron with gluons not only in the region of small  $z$  (Triple Regge Region) but also for  $z$  of the order of 1. This means that we extended the region of applicability to the complete region including large missing masses ( $M_X$ ) as well as small missing masses.

### 1. Splitting functions:

Before we go on with our discussion we should give the explicit expressions for the new splitting functions:

$$\begin{aligned}\Phi_P^F(z) &= \frac{1}{2N}16z^2(1-z) \\ \Phi_P^G(z) &= \frac{2N^2}{N^2-1}4z(1-z)^2\left(2+\frac{1}{z}\right)^2 \\ \bar{\Phi}_G^F(z) &= 3z(1-z)(2z-1)\end{aligned}\tag{2.25}$$

### 2. $G_{HT}$ -structure function :

The first two splitting functions were firstly derived in [?]. The third splitting function in eq. (2.25) is a modified Altarelli-Parisi splitting function. It is part of the third term in the square brackets of eq. (2.24) which we name  $G_{HT}$ -structure function. It was firstly introduced by Mueller and Qiu [?]. Our splitting function  $\bar{\Phi}_G^F$  is different compared to theirs due to the fact that they used the double multiperipheral cut to evaluate  $G_{HT}$  instead of the diffractive cut as we did. In our understanding the  $G_{HT}$ -contribution is beyond the leading order due to the extra factor  $\frac{k^2}{q^2}$  which results in some  $\log \ln \frac{q^2}{Q_0^2}$ . But, as we mentioned in the subsection before we are not allowed to neglect this contribution. We hope that the following short calculations will shed some light on the problem of this next to leading contribution.

The basic point in our approach is the fact that the integration over the transverse

momentum of the slowest produced parton has the form <sup>6</sup>:

$$\int_{|\bar{Q}_0^2|}^{|Q^2|} \frac{d|k^2|}{k^4} \quad (2.26)$$

Indeed, if, for example, out of  $n$  partons  $m$  are produced with smaller transverse momentum than  $k_t$  their contribution to the cross section turns out to be small. In LLA we would have to evaluate an integral of the type:

$$\alpha_s^n \int_{|\bar{Q}_0^2|}^{|Q^2|} \ln^{(n-m)} \left( \frac{Q^2}{k^2} \right) \ln^m \left( \frac{k^2}{\bar{Q}_0^2} \right) \frac{d|k^2|}{k^4} \quad (2.27)$$

The integral (2.27) yields

$$\frac{1}{|\bar{Q}_0^2|} \alpha_s^n \ln^{(n-m)} \left( \frac{Q^2}{\bar{Q}_0^2} \right) - \frac{1}{|Q^2|} \alpha_s^n B \ln^m \left( \frac{Q^2}{\bar{Q}_0^2} \right) \quad (2.28)$$

In the expression above we kept only the terms with the leading number of logs. Since  $|\bar{Q}_0^2| \ll |Q^2|$  the maximal answer will occur when  $m = 0$ . This means that we do not need to take into account the emission of gluons which are slower in their transverse momentum than  $k_t$ . However, if the whole sum of all logs  $\ln\left(\frac{k^2}{\bar{Q}_0^2}\right)$  leads to a function which is large (of the order  $\exp\left\{a\alpha_s \ln\left(\frac{k^2}{\bar{Q}_0^2}\right)\right\}$ ) we cannot trust the estimations above. In this case integral (2.27) is proportional to

$$\frac{1}{1 - a\alpha_s} \left\{ \frac{1}{|\bar{Q}_0^2|} \ln^{(n-m)} \left( \frac{Q^2}{\bar{Q}_0^2} \right) - \frac{1}{|Q^2|} \left( \frac{Q^2}{\bar{Q}_0^2} \right)^{a\alpha_s} \right\} \quad (2.29)$$

We can see that in the case of  $a\alpha_s > 1$  we need to take into account all contributions of the kind  $\ln\left(\frac{k^2}{\bar{Q}_0^2}\right)$ . Another example where the integral in eq. (2.24) does not dominate at the lower limit  $|\bar{Q}_0^2|$  but at the upper limit  $|Q^2|$  is given under point 4 in this subsection. We can summarize the situation in the following way: in a rough estimation of the cross section for diffractive dissociation we can neglect  $G_{HT}$  but for the sake of completeness and for the evolution equation we need to take into account this contribution.

There is one important shortcoming in the expression of  $G_{HT}$  in eq. (2.24) which we have not mentioned yet. It is valid only in the region of small  $z$  (Tripple Regge Region). That is why we put only  $\frac{1}{z}$  in front of the third term in eq. (1.24) and not the complete splitting function. We hope that in future we are able to improve the accuracy of our answer.

### 3. AGK-cutting rules:

---

<sup>6</sup>In order to simplify the discussion here we neglect any factor  $(1-z)$

Formula (2.24) allows us to check the AGK-cutting rules [?] using the result of Mueller and Qui [?]. They calculated the screening (shadowing) corrections to deep inelastic scattering in the double multiperipheral cut (both ladders are cut) assuming the validity of the AGK-cutting rules. The AGK-cutting rules in general say that the total diffractive cross section which includes the integration over  $|u_i^2|$  and  $\beta_u$  should be equal to the screening corrections with opposite sign. Fig. 2.3 shows graphically what the integration over  $\beta_u$  and  $|u_i^2|$  means. To perform this integration we need to specify the bottom vertex in fig. 2.3 in the same way as it was done in ref. [?].

It is easy to see from eq. (2.25) that the amplitude  $M$  which describes the interaction of the Pomeron with the proton is equal to

$$M(|u_i^2|) = \sum_{p^*} G_{pp^*}^2(|u_i^2|) \quad (2.30)$$

and does not depend on  $\beta_u$ .  $p^*$  denotes some state with the quantum numbers of the proton. All structure functions in eq. (2.24) do not depend on  $u_i^2$ . So, the integrated total cross section of the diffractive dissociation is proportional to

$$\int d|u_i^2| M(|u_i^2|) \quad (2.31)$$

To compare with the value of screening correction we do not need to specify eq. (2.31) because the same integral determines the value of screening corrections <sup>7</sup>. Finally the conclusion of the comparison is the following one:

A. In the case of the gluon-Pomeron vertex the AGK-cutting rules work and our answer coincides with that of Mueller and Qui (with opposite sign of course).

B. For the quark-Pomeron vertex, however, we got quite a different result. This means that AGK-cutting rules do not work in this case. We consider this result as very instructive but disappointing. A complete investigation of the AGK-cutting rules we prefer to postpone to a separate publication. We think that the observation we made here is very important and motivated us to present here the detailed calculations of the diffractive dissociation cross section including the discussion of all possible contributions to this process.

#### 4. Kinematical region $\frac{x}{\beta_u} \rightarrow 1$ :

It is very instructive to consider the cross section in the kinematical region  $\frac{x}{\beta_u} \approx 1$ . Here, we can integrate over  $|k^2|$  in eq. (2.24) without any additional cutoff  $|\overline{Q}_0^2|$ , or in other words, the natural cutoff turns out to be  $|\overline{Q}_0^2| \approx |Q^2|$  <sup>8</sup>. Indeed, in the region  $\frac{x}{\beta_u} \approx 1$  we

<sup>7</sup>detailed discussion on this subject see ref. [?] and appendix A.

<sup>8</sup>See ref. [?] where this problem was firstly discussed.

can use the following asymptotic expression:

$$D_F^F(z, |Q^2|, |k^2|) = \frac{\exp\{C_2(3 - 4\gamma_E)(\xi_Q - \xi_k)\}}{\Gamma[4C_2(\xi_Q - \xi_k)]} (1 - z)^{4C_2(\xi_Q - \xi_k) - 1}. \quad (2.32)$$

where  $\xi_k$  is defined as  $\xi_k = \frac{1}{b} \ln \ln(\frac{|k^2|}{\Lambda^2})$ . Inserting eq. (2.32) in eq. (2.24) yields

$$\begin{aligned} \frac{\beta_u d\sigma^{DD}(\gamma^*p \rightarrow Xp)}{d\beta_u d|u_t^2|} &= \sum_F \frac{4\pi^2 e_F^2 \alpha_{em}}{|Q^2| \Lambda^2} \frac{8\pi^2}{Nb} \int_{\frac{x}{\beta_u}}^1 dz \frac{z - \frac{x}{\beta_u}}{1 - z} \int_{\xi_{Q_0}}^{\xi_Q} d\xi_k \cdot \\ &\cdot \frac{\exp\{C_2[3 - 4\gamma_E + 4 \ln(1 - z)](\xi_Q - \xi_k) - 2b\xi_k - e^{b\xi_k}\}}{\Gamma[4C_2(\xi_Q - \xi_k)]} \cdot \\ &\cdot [\beta_u D_P^G(\beta_u, |k^2|, |Q_0^2|)]^2. \end{aligned} \quad (2.33)$$

One can see that in the region where  $\frac{x}{\beta_u}$  is very close to 1 the integration over  $\xi_k$  has a saddle point near to the upper bound  $\xi_Q$ .

This is one example how a natural scale for  $\overline{Q}_0^2$  could appear in our process. The only problem that we have is the accuracy of our approach, since in this kinematical region we cannot apply our selection of log contributions. In the integral over  $|k^2|$  not only small  $|k^2| \approx |\overline{Q}_0^2|$  are essential but also sufficiently large ones. We suspect that in this case not only the slowest partons have the spectrum  $\frac{dk^2}{k^4}$ . However in this kinematical region there is only a small number of produced secondary partons in the upper ladder of fig. 2.2. So here we are able to justify our approach.

##### 5. Evolution equation for the diffractive dissociation structure function:

Now, we would like to introduce a structure function which describes the contribution to the structure function of deep inelastic scattering due to diffractive dissociation at fixed mass  $M_X$ . Namely

$$\begin{aligned} D_{DD}^{F,G}\left(\frac{x}{\beta_u}, \beta_u, |Q^2|, |\overline{Q}_0^2|\right) &= \\ &= \int |G_p^{2G}(|u_t^2|)|^2 d|u_t^2| \int_{\frac{x}{\beta_u}}^1 \frac{dz}{z} \int_{\frac{|\overline{Q}_0^2|}{1-z}}^{|Q^2|} \frac{d|k^2|}{k^4} \frac{\alpha_s^2((1-z)|k^2|)}{16} \cdot \\ &\cdot \left[ \Phi_P^F(z) D_F^{F,G}\left(\frac{x}{\beta_u z}, |Q^2|, |k^2|\right) + \Phi_P^G(z) D_G^{F,G}\left(\frac{x}{\beta_u z}, |Q^2|, |k^2|\right) + \right. \\ &+ \left. \frac{8N^2}{N^2 - 1} \frac{|k^2|}{z} \int_{\frac{x}{\beta_u z}}^1 \frac{dz'}{z'} \int_{\frac{|k^2|}{1-z'}}^{|Q^2|} \frac{d|q^2|}{q^4} \frac{\alpha_s((1-z')|q^2|)}{4\pi} \overline{\Phi}_G^F(z') D_F^{F,G}\left(\frac{x}{\beta_u z z'}, |Q^2|, |q^2|\right) \right] \cdot \\ &\cdot [\beta_u D_P^G(\beta_u, |k^2|, |Q_0^2|)]^2. \end{aligned} \quad (2.34)$$

Differentiating equation (2.34) with respect to  $\ln(\frac{Q^2}{\Lambda^2})$  leads to the following evolution equations:

$$\begin{aligned}
& \frac{\partial}{\partial \ln(\frac{|Q^2|}{\Lambda^2})} q^{DD} \left( \frac{x}{\beta_u}, \beta_u, |Q^2|, |\bar{Q}_0^2| \right) = \\
& = \int_{\frac{x}{\beta_u}}^1 \frac{dz}{z} \frac{\alpha_s((1-z)|Q^2|)}{4\pi} \left[ \Phi_q^q(z) q^{DD} \left( \frac{x}{\beta_u z}, \beta_u, |Q^2|, |\bar{Q}_0^2| \right) \right. \\
& \quad \left. + \Phi_G^q(z) G^{DD} \left( \frac{x}{\beta_u z}, \beta_u, |Q^2|, |\bar{Q}_0^2| \right) \right] + \\
& \quad + \frac{\int |G_p^{2G}(|u_t^2|)|^2 d|u_t^2|}{|Q^2|} \left\{ \frac{\alpha_s^2 \left( \left(1 - \frac{x}{\beta_u}\right) |Q^2| \right)}{16} \Phi_P^q \left( \frac{x}{\beta_u} \right) \left[ \beta_u D_p^G \left( \beta_u, |Q^2|, |Q_0^2| \right) \right]^2 + \right. \\
& \quad \left. + \frac{8N^2}{N^2 - 1} \frac{\beta_u}{x} \int_{|\bar{Q}_0^2|}^{|Q^2|} \frac{d|k^2|}{|k^2|} \frac{\alpha_s^2(|k^2|)}{16} \int_{\frac{x}{\beta_u}}^{1 - \frac{k^2}{Q^2}} dz B \cdot \right. \\
& \quad \left. \cdot \frac{\alpha_s((1-z)|Q^2|)}{4\pi} \Phi_G^q(z) \left[ \beta_u G_p \left( \beta_u, |k^2|, |Q_0^2| \right) \right]^2 \right\} ; \tag{2.35}
\end{aligned}$$

$$\begin{aligned}
& \frac{\partial}{\partial \ln(\frac{|Q^2|}{\Lambda^2})} G^{DD} \left( \frac{x}{\beta_u}, \beta_u, |Q^2|, |\bar{Q}_0^2| \right) = \\
& = \int_{\frac{x}{\beta_u}}^1 \frac{dz}{z} \frac{\alpha_s((1-z)|Q^2|)}{4\pi} \left[ \Phi_q^G(z) q^{DD} \left( \frac{x}{\beta_u z}, \beta_u, |Q^2|, |\bar{Q}_0^2| \right) \right. \\
& \quad \left. + \Phi_G^G(z) G^{DD} \left( \frac{x}{\beta_u z}, \beta_u, |Q^2|, |\bar{Q}_0^2| \right) \right] + \\
& \quad + \frac{\int |G_p^{2G}(|u_t^2|)|^2 d|u_t^2|}{|Q^2|} \frac{\alpha_s^2 \left( \left(1 - \frac{x}{\beta_u}\right) |Q^2| \right)}{16} \Phi_P^G \left( \frac{x}{\beta_u} \right) \left[ \beta_u G_p^G \left( \beta_u, |Q^2|, |Q_0^2| \right) \right]^2 .
\end{aligned}$$

Here, we use the notation  $D_{DD}^F = q^{DD}$  and  $D_{DD}^G = G^{DD}$ . The functions  $\Phi_q^q$ ,  $\Phi_q^G$ ,  $\Phi_G^q$  and  $\Phi_G^G$  are the usual splitting functions in the GLAP-equation. The other splitting functions were defined in equation (2.25). Up to now we used  $|\bar{Q}_0^2|$  as lower bound of the transverse momentum squared  $|k_t^2|$ . In a simpler version of equation (2.35) we give  $|\bar{Q}_0^2|$  a new meaning actually as the starting virtuality of the evolution. Strictly speaking, since  $|k_t^2| = (1-z)|k^2|$ , this redefinition leads to a different result than we would get from equation (2.34) but within OB our approach this should not be too serious. In the same context we go back from  $|k_t^2|$  to  $|k^2|$  as argument of  $\alpha_s$ .

The two equations above now give the possibility to discuss the idea of Ingelman and Schlein [?] to introduce a Pomeron structure function which is simply the solution of the

usual GLAP-evolution equation with some special initial condition. At first glance on eq. (2.35) we conclude that it is impossible to introduce something like the structure function of the Pomeron. This becomes clear even by looking at eq. (2.34), since the structure function that corresponds to the Pomeron exchange ( $\beta_u D_p^G$ ) explicitly depends on the internal virtuality  $|k^2|$  and cannot be replaced by the flux of the Pomeron as it was done in ref. [?]. However, in the region of not extremely small  $\beta_u$  (see point 7) when the value of  $(\beta_u D_p^G)^2$  cannot compensate the factor  $\frac{1}{k^4}$  in the integral as well as not extremely small  $\frac{x}{\beta_u}$  (see point 4) we can see that the integration over  $|k^2|$  is concentrated at  $|k^2| \approx |\bar{Q}_0^2|$ . In this kinematical region we can replace  $\beta_u D_p^G(\beta_u, |k^2|, |Q_0^2|)$  by  $\beta_u D_p^G(\beta_u, |\bar{Q}_0^2|, |Q_0^2|)$  and define the Pomeron structure function as follows <sup>9</sup>:

$$\begin{aligned}
& D_P^{F,G} \left( \frac{x}{\beta_u}, |Q^2|, |\bar{Q}_0^2| \right) = \\
& = \frac{D_{DD}^{F,G} \left( \frac{x}{\beta_u}, \beta_u, |Q^2|, |\bar{Q}_0^2| \right)}{\left[ \beta_u D_p^G(\beta_u, |\bar{Q}_0^2|, |Q_0^2|) \right]^2} \frac{|\bar{Q}_0^2|}{\int |G_p^{2G}(|u_t^2|)|^2 d|u_t^2|} \frac{16}{\alpha_s^2(|\bar{Q}_0^2|)} \approx \\
& \approx |\bar{Q}_0^2| \int_{\frac{x}{\beta_u}}^1 \frac{dz}{z} \int_{|\bar{Q}_0^2|}^{|Q^2|} \frac{d|k^2|}{k^4} \frac{\alpha_s^2(|k^2|)}{\alpha_s^2(|\bar{Q}_0^2|)} \left[ \Phi_P^F(z) D_F^{F,G} \left( \frac{x}{\beta_{uz}}, |Q^2|, |k^2| \right) + \right. \\
& \quad \left. + \Phi_P^G(z) D_G^{F,G} \left( \frac{x}{\beta_{uz}}, |Q^2|, |k^2| \right) \right].
\end{aligned} \tag{2.36}$$

We have already neglected the  $G_{HT}$ -contribution. The main property of eq. (2.36) is the fact that the newdefined function only depends on the ratio  $\frac{x}{\beta_u}$  and not on  $\beta_u$  itself. Again we transform the integral equation above into a differential equation <sup>10</sup>:

$$\begin{aligned}
& \frac{\partial}{\partial \ln \left( \frac{|Q^2|}{\Lambda^2} \right)} q^P \left( \frac{x}{\beta_u}, |Q^2|, |\bar{Q}_0^2| \right) = \\
& = \frac{\alpha_s(|Q^2|)}{4\pi} \int_{\frac{x}{\beta_u}}^1 \frac{dz}{z} \left[ \Phi_q^q(z) q^P \left( \frac{x}{\beta_{uz}}, |Q^2|, |\bar{Q}_0^2| \right) + \Phi_G^q(z) G^P \left( \frac{x}{\beta_{uz}}, |Q^2|, |\bar{Q}_0^2| \right) \right] + \\
& + \frac{\bar{Q}_0^2}{Q^2} \frac{\alpha_s^2(|Q^2|)}{\alpha_s^2(|\bar{Q}_0^2|)} \Phi_P^q \left( \frac{x}{\beta_u} \right);
\end{aligned} \tag{2.37}$$

<sup>9</sup>Here we do not apply any of the standard definitions found in the literature [?, ?]. The definitions there were motivated phenomenologically with certain assumption on the Pomeron structure function. In our case we are just interested in the point how to simplify the diffractive dissociation structure function in order to apply the GLAP equation.

<sup>10</sup>We set  $D_P^F = q^P$  and  $D_P^G = G^P$ .

$$\begin{aligned}
& \frac{\partial}{\partial \ln\left(\frac{|Q^2|}{\Lambda^2}\right)} G^P\left(\frac{x}{\beta_u}, |Q^2|, |\overline{Q}_0^2|\right) = \\
& = B \frac{\alpha_s(|Q^2|)}{4\pi} \int_{\frac{x}{\beta_u}}^1 \frac{dz}{z} \left[ \Phi_q^G(z) q^P\left(\frac{x}{\beta_u z}, |Q^2|, |\overline{Q}_0^2|\right) + \Phi_G^G(z) G^P\left(\frac{x}{\beta_u z}, |Q^2|, |\overline{Q}_0^2|\right) \right] + \\
& + \frac{\overline{Q}_0^2}{Q^2} \frac{\alpha_s^2(|Q^2|)}{\alpha_s^2(|\overline{Q}_0^2|)} \Phi_P^G\left(\frac{x}{\beta_u}\right).
\end{aligned}$$

At first sight eq. (2.37) is still not the same as the GLAP equation that has been used in ref. [?]. However, within our accuracy we should neglect the last term in eq. (2.37) at large  $|Q^2|$ . The above equation then reduces to the GLAP equation with the specific initial conditions:

$$\begin{aligned}
\bar{q}^P\left(\frac{x}{\beta_u}, |\overline{Q}_0^2|, |\overline{Q}_0^2|\right) &= q^P\left(\frac{x}{\beta_u}, |\overline{Q}_0^2|, |\overline{Q}_0^2|\right) = \Phi_P^q\left(\frac{x}{\beta_u}\right); \\
G^P\left(\frac{x}{\beta_u}, |\overline{Q}_0^2|, |\overline{Q}_0^2|\right) &= \Phi_P^G\left(\frac{x}{\beta_u}\right).
\end{aligned} \tag{2.38}$$

It should be stressed that we do not need the energy sum rules

$$\int_0^1 dz z \left( q^P(z, |Q^2|, |\overline{Q}_0^2|) + G^P(z, |Q^2|, |\overline{Q}_0^2|) \right) = 1 \tag{2.39}$$

for the normalization of the Pomeron structure function. In our case this is done by equation (2.36) through the cutoff  $|\overline{Q}_0^2|$ . We finally have reduced the problem of evaluating the cross section for diffractive dissociation to the solution of the GLAP equation (2.37) with the initial condition (2.38) and its normalization due to eq. (2.36). The variables of the evolution procedure are  $\frac{x}{\beta_u}$  and  $|Q^2|$ .

The question is, now, what can we do if we are interested in the total cross section of diffractive dissociation including the region of integration over  $|k_t^2|$  below  $|\overline{Q}_0^2|$ . There we have to assume something about the contribution of jet production at small  $|k_t|$ . We think that the best we can do is to move to the "soft" Pomeron phenomenology with the experimental value  $G_{3P}$  as soon as  $|k_t|$  becomes smaller than 1 GeV. At  $|k_t| \approx \overline{Q}_0$  we can match our "hard" formulas with the phenomenological ones and extract the value of the natural cutoff  $\overline{Q}_0$  in eq. (2.36).

We can draw the conclusion that in the very rough approach where we neglect the contribution proportional to  $\frac{1}{|Q^2|}$  it is possible to introduce the deep inelastic structure function of the Pomeron with well defined initial conditions (2.38). But, at least when  $\frac{x}{\beta_u}$  reaches 1 we cannot believe in these initial conditions, since then the typical value of  $|k_t^2|$  in the master equation (2.24) approaches  $|Q^2|$ . In this case the eq. (2.37) gives an idea what change we

need to introduce for the structure function of the Pomeron. What happens when  $\beta_u$  comes very close to 0 will be discussed below.

### 6. *Experimental suggestion:*

We would like to note that we can introduce the sum

$$F_2^\Sigma(x, |Q^2|) = F_2(x, |Q^2|) + \int |G_p^{2G}(|u_t^2|)|^2 F_2^{DD} \left( \frac{x}{\beta_u}, \beta_u, |Q^2| \right) d\beta_u d|u_t^2| \quad (2.40)$$

where the second term is the integrated contribution to the diffractive dissociation structure function.

This sum has a very simple and remarkable property, namely, there are no screening corrections if the AGK-cutting rules are correct. It means that  $F_2^\Sigma$  obeys only the usual GLAP equation without any nonlinear term while each contribution separately has these screening corrections.

In some sense the experimental study of  $F_2^{DD}$  in comparison with  $F_2$  can give us the value of the screening corrections as well as a direct check of the AGK-cutting rules.

### 7. *Transverse momentum distribution of the slowest jet in the diffractive dissociation:*

As was noted in ref. [?] we have a different distribution over the transverse momentum of the slowest jet in the diffractive dissociation ( $k_t$  in fig. 2.2) in comparison with the distribution in a typical inelastic event in the deep inelastic scattering. It is easy to see directly from eq. (2.24) that

$$\begin{aligned} & \left. \frac{\beta_u d\sigma^{DD}}{d\beta_u d|u_t^2| d|k_t^2|} \right|_{|u_t^2| \ll |Q_0^2|} = \\ & = |G_p^{2G}(|u_t^2|)|^2 \sum_F \frac{4\pi^2 e_F^2 \alpha_{em}}{|Q^2|} \frac{\alpha_s^2(|k_t^2|)}{16} \frac{1}{k_t^4} \int_{\frac{x}{\beta_u}}^1 \frac{dz}{z} \frac{x}{\beta_u} (1-z) \cdot \\ & \cdot \left[ \Phi_P^F(z) D_F^F \left( \frac{x}{\beta_u z}, |Q^2|, \frac{|k_t^2|}{1-z} \right) + \Phi_P^G(z) D_G^F \left( \frac{x}{\beta_u z}, |Q^2|, \frac{|k_t^2|}{1-z} \right) + \right. \\ & + \frac{8N^2}{N^2-1} \frac{|k_t^2|}{z} \int_{\frac{x}{\beta_u z}}^1 \frac{dz'}{z'} \int_{\frac{|k_t^2|}{1-z'}}^{|Q^2|} \frac{d|q^2|}{q^4} \frac{\alpha_s((1-z')|q^2|)}{4\pi} \overline{\Phi}_G^F(z') D_F^F \left( \frac{x}{\beta_u z z'}, |Q^2|, |q^2| \right) \left. \right] \cdot \\ & \cdot \left[ \beta_u D_P^G \left( \beta_u, \frac{|k_t^2|}{1-z}, |Q_0^2| \right) \right]^2. \end{aligned} \quad (2.41)$$

The main factor here is  $\frac{1}{k_t^4}$  while the corresponding distribution in the deep inelastic scattering is proportional to  $\frac{1}{|k_t^2|}$ . So, we see that in diffractive dissociation the typical transverse momentum is much smaller than in the inelastic cross section of deep inelastic scattering

and the dependence on the lower cutoff is much stronger in diffractive dissociation than in deep inelastic scattering.

**8. Kinematical region  $\beta_u \rightarrow 0$  and  $x \rightarrow 0$ :**

Taking our master equation (2.24) again we would like to examine the region of small  $x_B$  ( $x_B$  is the Bjorken variable for which we use the notation  $x$ ) where  $\beta_u$  also goes to zero. We claim that in this region we leave the lower cutoff  $|\bar{Q}_0^2|$  and integrate over the complete region of  $|k^2|$ . This has already been discussed in the GLR-paper [?], but here we are going to stress some particular features of diffractive dissociation (see also [?]).

In order to illustrate all problems and properties of our process let us use the double log asymptotics for all our structure functions in eq. (2.24), namely

$$xG(x, |Q^2|, |k^2|) \sim \exp \left\{ \sqrt{16N(\xi_Q - \xi_k) \ln \left( \frac{1}{x} \right)} \right\} \quad (2.42)$$

$\xi_k$  is defined as  $\frac{1}{b} \ln \ln \left( \frac{|k^2|}{\Lambda^2} \right)$ . With this asymptotic expression the integral in (2.24) looks as follows:

$$\int_{\xi_{Q_0}}^{\xi_Q} d\xi_k \exp \left\{ -2b\xi_k - e^{b\xi_k} + \sqrt{16N(\xi_Q - \xi_k) \ln \left( \frac{\beta_u}{x} \right)} + 2\sqrt{16N(\xi_k - \xi_{Q_0}) \ln \left( \frac{1}{\beta_u} \right)} \right\} \quad (2.43)$$

The integration over  $z$  has no influence on the double log asymptotics and we can omit it here. Looking at eq. (2.43) we immediately see that there is a saddle point in the integration over  $\xi_k$ . Its value  $\xi_k^0$  can be found from the equation:

$$be^{b\xi_k^0} + \frac{1}{2} \sqrt{16N \frac{\ln \left( \frac{\beta_u}{x} \right)}{\xi_Q - \xi_k^0}} - \sqrt{16N \frac{\ln \left( \frac{1}{\beta_u} \right)}{\xi_k^0 - \xi_{Q_0}}} = 0 \quad (2.44)$$

There is one region

$$\xi_k^0 \ll \frac{1}{2b} \ln \left[ \frac{4N \ln \left( \frac{\beta_u}{x} \right)}{b^2 \xi_Q - \xi_k^0} \right] \quad (2.45)$$

where we can easily find the solution of eq. (2.44), namely

$$\xi_k^0 = \frac{4 \ln \left( \frac{1}{\beta_u} \right) \xi_Q + \ln \left( \frac{\beta_u}{x} \right) \xi_{Q_0}}{4 \ln \left( \frac{1}{\beta_u} \right) + \ln \left( \frac{\beta_u}{x} \right)} \quad (2.46)$$

Inserting this result in eq. (2.45) yields the kinematical region where eq. (2.46) is justified.

$$\frac{4 \ln \left( \frac{1}{\beta_u} \right) \xi_Q + \ln \left( \frac{\beta_u}{x} \right) \xi_{Q_0}}{4 \ln \left( \frac{1}{\beta_u} \right) + \ln \left( \frac{\beta_u}{x} \right)} \ll \frac{1}{2b} \ln \left[ \frac{4N \ln \left( \frac{\beta_u}{x} \right) + 4 \ln \left( \frac{1}{\beta_u} \right)}{b^2 \xi_Q - \xi_{Q_0}} \right] \quad (2.47)$$

This kinematical region corresponds to a missing mass squared  $M_X^2$  which is much larger than  $|Q^2|$  and a large value of  $|k^2|$  which is close to  $|Q^2|$ . The suppression with increasing  $|k^2|$  in this case is due to the structure function of the upper ladder and not due to the factor  $\frac{1}{k^4}$ . We have the compensation between the two lower ladders and the upper ladder. The opposite kinematical region is:

$$\xi_k^0 \gg \frac{1}{2b} \ln \left[ \frac{4N \ln \left( \frac{\beta_u}{x} \right)}{b^2 \xi_Q - \xi_{k_0}} \right] \quad (2.48)$$

With this condition we get the following equation for  $\xi_k^0$ :

$$\xi_k^0 + \frac{1}{2b} \ln[b(\xi_k^0 - \xi_{Q_0})] - \frac{1}{2b} \ln \left[ \frac{16N}{b} \ln \left( \frac{1}{\beta_u} \right) \right] = 0 \quad (2.49)$$

When we further restrict the region for  $\xi_k^0$  being

$$\frac{16N}{b^2} \ln \left( \frac{1}{\beta_u} \right) + \xi_{Q_0} \gg \xi_k^0 \gg \frac{1}{2b} \ln \left[ \frac{4N \ln \left( \frac{\beta_u}{x} \right)}{b^2 \xi_Q - \xi_{k_0}} \right] \quad (2.50)$$

we come to the solution

$$\xi_k^0 = \frac{1}{2b} \ln \left[ \frac{16N}{b} \ln \left( \frac{1}{\beta_u} \right) \right] \quad (2.51)$$

To be consistent in our estimations we have to fulfill the relation

$$\ln \ln \left( \frac{\beta_u}{x} \right) \gg \ln \ln \left( \frac{1}{\beta_u} \right) + \ln \left( 4b\xi_Q - 2 \ln \left[ \frac{16N}{b} \ln \left( \frac{1}{\beta_u} \right) \right] \right) \quad (2.52)$$

In the region that we are discussing now the missing mass  $M_X$  is, on the one hand side, much smaller than  $\sqrt{s}$ , on the other hand side, not extremely large compared to  $\sqrt{|Q^2|}$ . In this case the two lower ladder compensate the factor  $\frac{1}{k^4}$ .

Both solutions for  $\xi_k^0$  depend on  $\beta_u$ , i.e. the missing mass  $M_X$ , and as long as  $\beta_u$  is small enough we do not need a lower cutoff like  $|\bar{Q}_0^2|$  for  $|k^2|$ . I.e. the cross section of diffractive dissociation does not depend on  $|\bar{Q}_0^2|$ .

The first solution  $\xi_k^0$  in eq. (2.46) does not allow the definition of a Pomeron structure function in the sense of eq. (2.36) because  $\xi_k^0$  depends on and  $|Q^2|$ . The second saddle point solution (2.51), however, only depends on  $\beta_u$  and provides us with a new scale  $|k_0^2|$  which serves as starting point for our evolution equation (2.37). Eq. (2.51) leads to the following expression for  $|k_0^2|$ :

$$|k_0^2| = \Lambda^2 \exp \left[ \sqrt{\frac{16N}{b} \ln \left( \frac{1}{\beta_u} \right)} \right] \quad (2.53)$$

As before  $q^P$  and  $G^P$  denote the solution of the evolution equation (2.37) together with the initial condition (2.38). The normalization has to be changed including the width of the saddle now. The diffractive dissociation structure function turns out to be:

$$q^{DD} \left( \frac{x}{\beta_u}, \beta_u, |Q^2| \right) = q^P \left( \frac{x}{\beta_u}, \beta_u, |Q^2| \right) \sqrt{2\pi} \left\{ \left[ 1 + \frac{1}{2 \ln \left( \frac{\ln \left( \frac{|k_0^2|}{\Lambda^2} \right)}{\ln \left( \frac{|Q_0^2|}{\Lambda^2} \right)} \right)} \right] b^2 \ln \left( \frac{|k_0^2|}{\Lambda^2} \right) \right\}^{-\frac{1}{2}} \cdot \frac{\int |G_p^{2G}(|u_t^2|)|^2 d|u_t^2| \alpha_s(|k_0^2|)}{|k_0^2| 16} [\beta_u D_p^G(\beta_u, |k_0^2|, |Q_0^2|)]^2 ; \quad (2.54)$$

$$G^{DD} \left( \frac{x}{\beta_u}, \beta_u, |Q^2| \right) = G^P \left( \frac{x}{\beta_u}, \beta_u, |Q^2| \right) \sqrt{2\pi} \left\{ \left[ 1 + \frac{1}{2 \ln \left( \frac{\ln \left( \frac{|k_0^2|}{\Lambda^2} \right)}{\ln \left( \frac{|Q_0^2|}{\Lambda^2} \right)} \right)} \right] b^2 \ln \left( \frac{|k_0^2|}{\Lambda^2} \right) \right\}^{-\frac{1}{2}} \cdot \frac{\int |G_p^{2G}(|u_t^2|)|^2 d|u_t^2| \alpha_s(|k_0^2|)}{|k_0^2| 16} [\beta_u D_p^G(\beta_u, |k_0^2|, |Q_0^2|)]^2 .$$

The equation above reveals the strong dependence on the proton structure function  $D_p^G$  whereas the evolution from  $|k_0^2|$  to  $|Q^2|$  turns out to be a small correction which we even neglected while evaluating the saddle point (passing from eq. (2.44) to eq. (2.51)).

So far we assumed the simple double leading log asymptotics for the proton structure function which has to be modified by taking into account shadowing (screening) corrections. These corrections correspond to diagrams shown in fig. 2.4 which were summed by the nonlinear evolution equation (GLR-equation, see ref. [?, ?]). Since the GLR-equation only gives the possibility to calculate the structure function in the region where the shadowing corrections are still small, we need for very small  $\beta_u$  some additional hypothesis, the so called parton density saturation hypothesis.

$$\beta_u D_p^G(\beta_u, |k^2|, |Q_0^2|) = \begin{cases} a \frac{|k^2|}{q_0^2(\beta_u)} & \text{for } |k^2| < q_0^2(\beta_u) \\ a \frac{q_0^2(\beta_u)}{|k^2|} & \text{for } |k^2| > q_0^2(\beta_u) \end{cases} \quad (2.55)$$

where  $q_0^2(\beta_u)$  is equal to (see [?, ?])

$$q_0^2(\beta_u) = Q_0^2 + \Lambda^2 \exp \left\{ 3.56 \sqrt{\ln \left( \frac{\beta_0}{\beta_u} \right)} \right\} . \quad (2.56)$$

In the framework of the saturation hypothesis we can calculate the total cross-section of diffractive dissociation. It is easy to see that using eq. (2.55) the integral over  $|k^2|$  in eq. (2.24) is convergent and takes the form <sup>11</sup>

$$\begin{aligned}
& \frac{\beta_u d\sigma^{DD}}{d\beta_u d|u_t^2|} (\gamma^* p \rightarrow X p') \Big|_{|u_t^2| \ll |Q_0^2|} = \\
& = |G_p^{2G}(|u_t^2|)|^2 \sum_F \frac{4\pi^2 e_F^2 \alpha_{em}}{|Q^2|} \frac{4}{3} \frac{a^2}{q_0^2(\beta_u)} \int_{\frac{x}{\beta_u}}^1 \frac{dz}{z} \frac{x}{\beta_u} \frac{\alpha_s^2(q_0^2(\beta_u))}{16} . \\
& \cdot \left[ \Phi_P^F(z) D_F^F \left( \frac{x}{\beta_u z}, |Q^2|, q_0^2(\beta_u) \right) + \Phi_P^G(z) D_G^F \left( \frac{x}{\beta_u z}, |Q^2|, q_0^2(\beta_u) \right) \right] .
\end{aligned} \tag{2.57}$$

In this kinematical region we can introduce the structure function of the Pomeron using eq. (2.36) with  $\bar{Q}_0^2 = q_0^2(\beta_u)$ . For this structure function again we can apply the usual GLAP evolution equation with the initial condition (2.38).

At the end of this section we have to discuss another type of corrections. These are emissions below the cell in which we have  $\frac{d|k^2|}{k^4}$  integration (see fig. 2.5). This extra contribution is similar to  $G_{HT}$  that we have discussed under point 2. It is not suppressed by any power of  $\alpha_s$  [?, ?], but it turns out [?] that due to the colour structure of QCD the emission of gluons below the cell with  $\frac{d|k^2|}{k^4}$  integration are proportional to  $\frac{1}{N^2-1}$ . This factor is numerical small and we do not take into account the corresponding contribution. In ref. [?] such contributions were investigated in detail and it was shown that we have to multiply our answer (eq. 2.24) by a factor

$$R^2 = B \exp \left\{ \delta \sqrt{16N \ln \left( \frac{1}{\beta_u} \right) (\xi_k - \xi_{Q_0})} \right\} \tag{2.58}$$

with  $\delta \approx 10^{-2}$  for  $N = 3$ . One can directly conclude from equation (2.58) that such emission give negligible contribution for any reasonable value of  $\ln \left( \frac{1}{\beta_u} \right)$ .

### 3 Photon diffractive dissociation at Born-level:

This section is devoted to the technical details of the calculation of the diffractive dissociation cross section at Born- level. The next section will include the generalization to higher order of perturbation theory.

Due to the fact that the photon couples to quarks only (and not to gluons) the minimal configuration of the diffractive dissociation process is the dissociation into two quark-jets

---

<sup>11</sup>We have neglected the  $G_{HT}$  contribution because it is beyond our approach here.

(quark and anti-quark) (fig 3.1). The next step towards the complete description of photon diffractive dissociation is the inclusion of one gluon-jet (fig. 3.7). These two cases serve as starting point for the generalization.

### 3.1 Photon diffractive dissociation into two jets:

Since photon diffractive dissociation is part of the general deep inelastic scattering, another name for our process could be diffractive deep inelastic scattering. New in the case of diffractive dissociation is the more exclusive final state which contains the proton only slightly scattered. The rest of the particles in the final state (here quark and anti-quark) take the quantum numbers of the photon. The quarks and the proton are well separated in rapidity provided that the missing mass  $M_X$  (invariant mass of the two quarks) is much smaller than the c.m.s.-energy  $\sqrt{s}$ . Naturally,  $|Q^2| < M_X^2$ <sup>12</sup> so that all our discussion is restricted to a small x-Bjorken ( $x_B \equiv x$  in our notation). In this region the leading contribution to the cross-section comes from the Pomeron-exchange. At Born-level and in the framework of QCD the Pomeron is represented by a pair of gluons in the colour singlet state.

Fig. 3.1, now, shows all the diagrams which have to be taken into account. Gauge invariance requires a set of diagrams which includes all permutations of the photon and the two gluon lines. Diagrams with crossed gluon lines were not explicitly shown in fig. 3.1, instead each single diagram represents the sum of two diagrams with and without crossed gluon lines. We do this because summing the crossed and uncrossed diagram (s-channel and u-channel contribution) results in the approximate cancellation of the real part of these two diagrams. Only the imaginary part is left.

The momentum  $u$  which is transferred along the two gluons was already introduced in section 2. For simplicity we set  $u^2$  which is the momentum transfer  $t$  equal to zero. This assumption is realistic, since the proton's form factor decreases strongly with increasing  $t$ . In the following discussion we further assume that the two gluons couple to a quark instead of the proton in the lower part of the diagram. The scattering of the Pomeron on the proton is given in appendix A.

Before we start the explicit calculation we should mention that a similar calculation has been done by Ryskin [?]. While checking his result we found some mistake and present here the correct answer. Nikolaev and Zakharov [?], too, have calculated this process but used a different technique. It is possible to transform their result into ours. The main difference in the technique is that we apply the Leading Log Approximation which allows the generalization to higher order perturbation theory which we are interested in.

Since our approach is based on the Leading Log Approach we concentrate on the region

---

<sup>12</sup> $|Q^2|$  could be interpreted as the mass of the incoming photon

of integration over  $|l_t^2|$  (see fig. 3.1) which yields some log in  $|\overline{Q}_0^2|$ . This requires the strong ordering of the transverse momenta (for notation see fig. 3.1):

$$|Q^2| \gg |k_t^2| \gg |l_t^2| \gg |u_t^2| \approx 0 \quad (3.1)$$

The  $\alpha_l$  component of the momentum  $l$  (we use Sudakov variables:  $l = \alpha_l Q' + \beta_l p + l_t$ ) is fixed by taking the pole of the propagator  $p - u - l$ , whereas  $\alpha_u$  and  $\alpha_k$  are fixed using the mass-shell condition of the final states with the momenta  $p - u$  and  $k - u$ . The third mass-shell condition (momentum  $k + Q$ ) serves to fix  $\beta_k$ .

We, now, come back to the point where we need the crossing of the gluons (crossing in the t-channel, fig. 3.2). As we already mentioned taking the sum of the crossed and uncrossed diagram is equivalent to the sum of the s-channel and u-channel contribution. Due to the positive signature of our diagrams (colour singlet state) we know that the real part cancels out, at least in the leading order neglecting terms proportional to  $\frac{M_X^2}{s}$ . The remaining imaginary part of each diagram in fig. 3.1 is given by the imaginary part of the propagator  $k - l - u$  and  $k + Q + l$  respectively. In order to evaluate this imaginary part we just have to substitute a  $\delta$ -function for each propagator. It is important to remark that each  $\delta$ -function is accompanied by one  $\pi$  and not  $2\pi$  as usually appears while taking the pole of some propagator. We can say that due to the smallness of the momentum  $u$  the amplitude is approximately equal to the half of its discontinuity.

We have already mentioned that in our approach we set  $t$  equal to zero. It follows that  $u_t$  and  $\alpha_u$  are zero, too. This means that the momentum  $u$  has only one component along  $p$ ,  $u = \beta_u p$ .  $\beta_u$  can be expressed in terms of the missing mass  $M_X$  and  $|Q^2|$ :

$$\begin{aligned} M_X^2 &= (Q + u)^2 \\ \Rightarrow \beta_u &= \frac{M_X^2 + |Q^2|}{s} \end{aligned} \quad (3.2)$$

We now give a table of all kinematical relations which we have discussed so far:

$$\begin{aligned} \alpha_l &= \frac{l_t^2}{s}; \\ \alpha_u &= \frac{u_t^2}{s} = 0; \\ \alpha_k &= \frac{k_t^2}{(\beta_u - \beta_k)s}; \\ a) \beta_l &= \frac{l_t^2 - 2(l_t, k_t)}{\alpha_k s}; & b) \beta_l &= 0; \\ \beta_k &= x; \\ \beta_u &= \frac{M_X^2}{s} + x; \end{aligned} \quad (3.3)$$

$$u^2 = u_t^2 = t = 0 .$$

For  $\beta_l$  we have two different results: eq. a) belongs to diagram 3.1.a and 3.1.c and eq. b) to diagram 3.1.b and 3.1.d. From table (3.3) it is clear together with eq. (3.1) that all  $\alpha$ -variables are strongly ordered:

$$1 \gg |\alpha_k| \gg |\alpha_l| \gg |\alpha_u| = 0 \quad (3.4)$$

We would like to illustrate this in the case of  $|\alpha_k|$  and  $|\alpha_l|$ . There are two reasons why these two variables are strongly ordered. The first is that we assumed  $|k_t^2| \gg |l_t^2|$  and the second one is the smallness of  $x$  and  $\beta_u$ :  $\beta_u - x = \frac{M_x^2}{s} \ll 1$ . So, even if  $l_t$  is not much smaller than  $k_t$ ,  $\alpha_l$  is small compared to  $\alpha_k$  and we are allowed to neglect it. This neglect we have already used while calculating  $\beta_l$  in table (3.3).

After having clarified the kinematical situation we proceed with the calculation of the lower part of the diagrams in fig. 3.1. In each diagram the pair of gluons is radiated by a very fast moving quark <sup>13</sup>. The gluons are sufficiently soft ( $\frac{M_x^2}{s} \ll 1$ ) and the emission could be understood as virtual Bremsstrahlung. In the language of Feynman rules this means that we can use the eikonal approximation. For example:

$$\bar{u}(p-u)\gamma^\sigma(\hat{p}-\hat{l}-\hat{u})\gamma^\rho u(p) \approx 4 p^\sigma p^\rho \bar{u}(p)u(p) \quad (3.5)$$

All other contributions turn to be beyond the leading order that we are interested in. We see that the gluons are polarized along  $p$ . So far we have not specified the gauge. If we assumed the Feynman gauge, the polarization vector  $p^\sigma$  of each gluon would be directly transmitted to the top of the diagram. With this  $p$ -vector we could go on calculating the upper fermion-line, but instead we prefer to use a trick which will help us to reduce the number of diagrams which actually have to be calculated. Fig. 3.3 shows that we can isolate out of the diagrams 3.1.a and 3.1.c a gauge invariant substructure. Gauge invariance is guaranteed because the quark with the momentum  $k-l-u$  is on mass-shell ( $(k-l-u)^2 = 0$ ). Let us call the upper part of fig. 3.3, where the gluon is coupled to,  $M^\rho$ . Then

$$(l+u)_\rho M^\rho = 0 \quad \Rightarrow \quad p_\rho M^\rho = -\frac{l_{t\rho}}{\beta_l + \beta_u} M^\rho . \quad (3.6)$$

We neglected  $\alpha_l$  as well as  $u_t$ . Eq. (3.6) is generally known as Ward identity. In appendix B.1 we show how this result is reached by summing explicitly the two diagrams in fig. 3.3. Using the polarization  $-\frac{l_{t\rho}}{\beta_l + \beta_u}$  instead of  $p^\rho$  allows to neglect the diagram in fig. 3.3.b because its contribution is proportional to  $\frac{(l_t, k_t)}{s}$ .

---

<sup>13</sup>we work in the Breit-frame

A further possibility usually used to calculate the Altarelli- Parisi splitting function is the use of the light cone gauge with  $Q'$  as gauge vector ( $A \cdot Q' = 0$ ). In this gauge the propagator looks as follows ( $k$  is any vector):

$$\frac{-id^{\mu\nu}(k)}{k^2} \quad (3.7)$$

with

$$d^{\mu\nu}(k) = g^{\mu\nu} - \frac{k^\mu Q'^\nu + Q'^\mu k^\nu}{(k, Q')} . \quad (3.8)$$

Multiplying  $d^{\mu\nu}(k)$  by  $p_\mu$  directly yields  $-\frac{k^\nu}{\beta_k}$  where we neglected  $\alpha_k Q'^\nu$ . For the right gluon in the diagrams 3.1 which carries the momentum  $l$  we keep p-polarization.

We finally come to the conclusion that we only need to evaluate the diagrams in fig. 3.1.a and 3.1.b, whereas those in 3.1.c and 3.1.d do not contribute provided we use as polarization vector for the left gluon  $-\frac{l_t^\rho}{\beta_l + \beta_u}$ .

We go on with the evaluation of the upper fermion line in fig. 3.1.a. and 3.1.b.

$$-\bar{u}(k+Q) \gamma_{t_\mu} \frac{\hat{k}}{k^2} \frac{\hat{l}_t}{\beta_l + \beta_u} (\hat{k} - \hat{l} - \hat{u}) \hat{p} v(u-k) \frac{\pi}{\alpha_k s} \quad (3.9)$$

$$\bar{u}(k+Q) \hat{p} (\hat{k} + \hat{Q} + \hat{l}) \gamma_{t_\mu} \frac{\hat{k} + \hat{l}}{(k+l)^2} \frac{\hat{l}_t}{\beta_l + \beta_u} v(u-k) \frac{\pi}{s} .$$

Since we consider only transverse polarized photons, we introduced in eq. (3.9)  $\gamma_{t_\mu}$  instead of  $\gamma_\mu$  for the photon vertex. The factor  $\frac{\pi}{\alpha_k s}$  and  $\frac{\pi}{s}$  in eq. (3.9) is the result of integrating the  $\delta$ -functions which have to be introduced in order to calculate the imaginary part of the amplitude as explained above.

Both expressions in eq. (3.9) have to be expanded to the order  $\frac{l_t^2}{k_t^2}$ , for we would like to extract the log over  $l_t^2$ . The details how to proceed is given in appendix B.1. The result for both expressions in eq. (3.9) is

$$2z(1-z) \bar{u}(k+Q) \gamma_{t_\mu} v(u-k) \frac{\pi l_t^2}{\beta_u k_t^2} . \quad (3.10)$$

The variable  $z$  is defined as  $z = \frac{\beta_k}{\beta_u} = \frac{x}{\beta_u}$ .

Next, we would like to evaluate the colour coefficient of the diagrams in fig. 3.1. This is easy to do, for the pair of gluons is assumed to make up a colour singlet state. Fig. 3.4 shows how this looks graphically. We only have to deal with a gluon loop which is attached to a fermion line as shown in fig. 3.5. The result is simply:

$$\frac{C_F}{N^2 - 1} = \frac{1}{2N} \quad (3.11)$$

We would like to conclude this subsection with the complete expression for the cross section of photon diffractive dissociation at Born-level (see fig. 3.6):

$$\left. \frac{\beta_u}{d\beta_u} \frac{d\sigma}{dt} \right|_{t=0} = \sum_F \frac{4\pi^2 \alpha_{em} e_F^2}{|Q^2|} \int_{\frac{|\overline{Q}_0^2|}{1-z}}^{|\overline{Q}^2|} \frac{d|k^2|}{k^4} \frac{\alpha_s^2}{16} \frac{8}{N} z^2(1-z) \left( 4C_F \int_{|\overline{Q}_0^2|}^{|\overline{Q}^2|} \frac{d|l_t^2|}{|l_t^2|} \frac{\alpha_s}{4\pi} \right)^2 \quad (3.12)$$

We remind the reader that a factor  $\frac{1}{4}$  is due to averaging over the polarizations of the incoming quark and transverse photon.  $|Q_0^2|$  is as usual the initial virtuality of the quark in the proton. We already introduced the value  $|\overline{Q}_0^2|$  as lower cutoff for the transverse momentum squared  $k_t^2$  in section 2. It should be large enough first of all to justify perturbative QCD and second to give room for some evolution from  $|Q_0^2|$  to  $|\overline{Q}^2|$ . The relation between the virtuality  $|k^2|$  and the transverse momentum squared  $|k_t^2|$  is given by  $|k_t^2| = (1-z)|k^2|$ .

As was noted before, expression (3.12) could be derived from the result of Nikolaev and Zakharov [?] by passing to the Leading Log Approximation. Nikolaev and Zakharov did not introduce something like  $\overline{Q}_0^2$  but used instead of that the quark mass  $m_f$  as lower cutoff. <sup>14</sup> As can be seen from eq. (3.12) for large masses  $M_X$  we have a spectrum of the type:

$$\frac{d\sigma}{dt dM_X^2} \approx \frac{Q^4}{|\overline{Q}_0^2| M_X^8} \quad (3.13)$$

This equation shows that our leading log result is strongly suppressed at large  $M_X$ . In this region the main contribution comes from a pointlike Pomeron, and the formula of Nikolaev and Zakharov gives the correct answer:

$$\frac{d\sigma}{dt dM_X^2} \approx \frac{1}{m_f^2 M_X^4} \quad (3.14)$$

One would expect such a type of spectrum, for the Pomeron acts as a pointlike particle similar to a gluon or photon and we are left with only one quark exchange in the region of the t-channel where the two quark-jets are produced (see for example fig. 3.6). We would like to stress that eq. (3.14) does not contradict our result, it is just outside the region where the Leading Log Approximation is applicable.

### 3.2 Photon diffractive dissociation into three jets:

On the way to some complete expression for the cross section of diffractive dissociation we have to investigate the case when besides the two quark jets one additional gluon jet is emitted.

---

<sup>14</sup>We neglect all quark masses.

Before we look at all the diagrams which may contribute we have to specify in which gauge we would like to work. In contrast to Ryskin [?] we use the light cone gauge with  $Q'$  as gauge vector ( $(A, Q') = 0$ ). We think that in this gauge it is more convenient to calculate the diagrams in the kinematical region where  $\beta_u$  could be of the same order as  $x$ . This gauge can also be used to derive the Altarelli-Parisi splitting functions in a similar way as was done by DDT [?].

We have already introduced the corresponding propagator (see (3.7) and (3.8)) which is

$$\frac{-id^{\mu\nu}(r)}{r^2} \quad (3.15)$$

with OB

$$d^{\mu\nu}(r) = g^{\mu\nu} - \frac{r^\mu Q'^\nu + Q'^\mu r^\nu}{(r, Q')} . \quad (3.16)$$

$r$  can be any momentum. Apart from the propagator we need the polarization vector of a real gluon, i.e. a gluon on mass-shell:

$$\epsilon^\mu(r) = \epsilon_t^\mu(r) - \frac{(r_t, \epsilon_t(r))}{(r, Q')} Q'^\mu \quad (3.17)$$

$\epsilon_t(r)$  denotes a vector in the transverse momentum plane which has the following properties:

$$\begin{aligned} (\epsilon_t(r), \epsilon_t(r)) &= -1 ; \\ \sum_{\text{Pol}} \epsilon_t^\mu(r) \epsilon_t^\nu(r) &= -g_t^{\mu\nu} . \end{aligned} \quad (3.18)$$

Since the transverse plane is two-dimensional we only need two basic polarization vectors. When we sum over the polarizations as in eq. (3.18) we actually sum over these basic polarization vectors. In practice we only need the second relation in (3.18).

The kinematical situation is similar to that in the previous subsection. We have strong ordering in the transverse momenta and the  $\alpha$ - components:

$$\begin{aligned} |Q^2| \gg |q_t| \gg |k_t^2| \gg |l_t^2| \gg |u_t^2| = 0 ; \\ 1 \gg |\alpha_q| \gg |\alpha_k| \gg |\alpha_l| \gg |\alpha_u| = 0 . \end{aligned} \quad (3.19)$$

As lower cutoff for  $|k_t^2|$  we will assume  $|\overline{Q}_0^2|$ , whereas for  $|l_t^2|$  we have the usual  $|Q_0^2|$ . The mass-shell conditions (see fig. 3.7) including the poles of the propagator  $p-l-u$ ,  $k-l-u$  as well as  $q-l-u$  lead to the following table of kinematical relations:

$$\alpha_q = \frac{q_t^2}{(\beta_k - \beta_q)s} ;$$

$$\begin{aligned}
\alpha_k &= \frac{k_t^2}{(\beta_u - \beta_k)s}; \\
\alpha_l &= \frac{l_t^2}{s}; \\
\alpha_u &= \frac{u_t^2}{s} = 0; \\
\beta_q &= x; \\
a) \beta_l &= \frac{l_t^2 - 2(l_t, k_t)}{\alpha_k s}; & b) \beta_l &= 0; \\
\beta_u &= \frac{M_X^2}{s} + x; \\
u^2 = u_t^2 &= t = 0.
\end{aligned} \tag{3.20}$$

Here again we used the fact that the imaginary part of our diagrams dominate over the real part. The variable  $\beta_k$ , now, has to be integrated. It ranges from  $\beta_u$  down to  $x$ .

### 3.2.1 Higher twist $\frac{1}{k^4}$ :

In this part of the current subsection we restrict ourselves to the case where we have a logarithmic integration over  $|q^2|$  instead of  $|k^2|$ . The latter case which we usually call the 'next to leading order' will be investigated afterwards. The restriction just mentioned demands that each amplitude has to be proportional to  $\frac{q_t^4}{q_t^2}$ . The first order  $q_t$  in the numerator originates from the gluon-quark vertex and the denominator  $\frac{1}{q_t^2}$  from the quark propagator. In analogy to the subsection before we are going to extract the logarithmic contribution over  $l_t^2$  from all diagrams.

The variety of diagrams which may contribute is quite large, now. But the specific choice of the gauge and the fact that we are only interested in terms proportional to  $l_t^2$  reduce their number. The gauge that we chose allows to neglect diagrams with real gluon emission from their top, i.e. emission from the upper fermion line, whereas emission from the bottom gives some contribution. The light cone gauge with  $p$  as gauge vector ( $(p, A) = 0$ ) has the opposite effect (see ref. [?]). There, the emission from the bottom can be neglected.

We conclude that it is enough to calculate the set of diagrams given in fig. 3.7 and 3.8. One example of diagrams which do not contribute is shown in fig. 3.9. It yields a contribution which is proportional to  $\frac{l_t^4}{l_t^4}$ . The details of the calculation we leave for the appendix and present here only the final answer and some general remarks.

We divided up the complete set of diagrams into two groups, fig. 3.7 and 3.8. The difference between them is, roughly speaking, the fact that in fig. 3.7 we have an interaction

in the final state between the gluon and the bottom quark whereas in fig. 3.8 the common property is the interaction between the quark pair at the top and the bottom quark. One could object that the diagram in fig. 3.7.b does not perfectly fit into this group but the final answer suggests to put it there because, then, the result of all diagrams in fig. 3.7 is the same as in fig. 3.8.

The polarization vector of all the gluons which are emitted from the bottom line are aligned along the momentum  $p$ . If we multiply now the vector  $p^\rho$  by  $d^{\rho\mu}(l+u)$  we get  $-\frac{l^\rho}{\beta_l+\beta_u}$ . For the second lower t-channel gluon with momentum  $l$  it turns out to be more convenient to keep the p-polarization. This is possible, since the lines on the right and on the left to the point where this gluon is attached are on mass-shell except in diagram 3.7.b. The 'local' gauge invariance allows us to change the gauge. In diagram 3.7.b we have this possibility, too, but now, at the top where the right t-channel gluon couples to the quark line. The quarks on both sides of the vertex are on mass-shell again. The numerator of the propagator  $l+u-k$  can be changed from

$$\frac{Q^\nu(k_t-l_t)^\mu}{(\beta_l+\beta_u-\beta_k)(p,Q')} \quad (3.21)$$

to

$$\frac{Q^\nu p^\mu}{(p,Q')} \quad (3.22)$$

The t-channel gluons on which we focus at the moment (so called Coulomb gluons) have a specific property: due to the fact that they couple to two particles on mass-shell their  $\beta$ -components turn out to be small, i.e. they are very soft. The smallness of the  $\beta$ -component allows us to use the approximate form (3.21) instead of  $d^{\nu\mu}(l+u-k)$ .

Another important property of these soft gluons is the fact that they feel the total charge of the quark anti-quark pair and not its substructure. This may be illustrated with the help of the following example (see diagram 3.8.a):

$$\frac{(\hat{q}-\hat{l}-\hat{k})\hat{p}v(k-q)}{\alpha_{qs}} \approx v(k-q) \quad (3.23)$$

The  $\alpha_{qs}$  in the denominator is the residue of the propagator  $q-l-k$  in connection with the integration over  $\beta_l$ . The eq. (3.23) only holds if we demand to have a logarithmic integration over  $q_t^2$ <sup>15</sup>. Taking into account the second quark with a similar approximation as in eq. (3.23) the colour of both quarks add up to the colour of the left gluon. The approximation which was used in eq. (3.23) we already know from the gluon-emission at the

---

<sup>15</sup>For the sake of completeness we should add a minus to eq. (3.23) due to the direction of the fermion line (incoming).

bottom, it is the eikonal approximation. This type of approximation is intimately related to the classical current emission (see [?, ?]).

The previous discussion and its application gives a great simplification in the calculation of all diagrams in fig. 3.7 and 3.8. The total colour structure becomes easy to handle and can be reduced to the structure in fig. 3.10. Due to the colour singlet state of the lower gluon pair the colour coefficient in fig. 3.7.b is the negative of the colour coefficient in fig. 3.7.a. The colour coefficient of diagram 3.7.c and 3.7.d add up to give again the same as in diagram 3.7.a and in a similar way all diagrams of fig. 3.8 can be normalized to diagram 3.7.a.

The amplitude which finally represents the sum of all diagrams in fig 3.7 and 3.8 is proportional to

$$\begin{aligned}
& -eg_s^3 \frac{\pi}{\beta_u k^2} \frac{N}{N^2 - 1} T_{ij}^a \bar{u}(q + Q) \gamma_{t\mu} \frac{\hat{q}}{q^2} \hat{e}_t(u - k) v(k - q) \cdot \\
& \cdot 2(1 - z)(2 + \frac{1}{z}) 4C_F \int_{Q_0^2}^{k^2} \frac{d|l_t^2|}{|l_t^2|} \frac{\alpha_s}{4\pi} .
\end{aligned} \tag{3.24}$$

$z$  is defined as  $\frac{\beta_k}{\beta_u}$ . The indices  $a$ ,  $i$  and  $j$  are the colour indices of the gluon, quark and anti-quark. Over the colours of the incoming quark we averaged.

To complete the discussion we give the cross section of the three jet event (see fig. 3.11)

$$\begin{aligned}
\left. \frac{\beta_u d\sigma}{d\beta_u dt} \right|_{t=0} &= \sum_F \frac{4\pi^2 \alpha_{em} e_F^2}{|Q^2|} \int_{\frac{x}{\beta_u}}^1 \frac{dz}{z} \frac{x}{\beta_u} \int_{\frac{|Q_0^2|}{1-z}}^{|Q^2|} \frac{d|k^2|}{k^4} \frac{\alpha_s^2}{16} \int_{|k^2|}^{|Q^2|} \frac{d|q^2|}{|q^2|} \frac{\alpha_s}{4\pi} \cdot \\
& \cdot \left\{ \Phi_G^F \left( \frac{x}{z\beta_u} \right) \Phi_P^G(z) + \Phi_F^F \left( \frac{x}{\beta_u z} \right) \Phi_P^F(z) \right\} \left( 4C_F \int_{|Q_0^2|}^{k^2} \frac{d|l_t^2|}{|l_t^2|} \frac{\alpha_s}{4\pi} \right)^2
\end{aligned} \tag{3.25}$$

and define two Pomeron splitting functions, the first one describes the Pomeron splitting into two gluons and the second one the splitting into two quarks:

$$\begin{aligned}
\Phi_P^G(z) &= \frac{2N^2}{N^2 - 1} 4z(1 - z)^2 \left(2 + \frac{1}{z}\right)^2 \\
\Phi_P^F(z) &= \frac{1}{2N} 16z^2(1 - z)
\end{aligned} \tag{3.26}$$

$\Phi_G^F$  and  $\Phi_F^F$  are the usual Altarelli-Parisi splitting functions. The first one stands for the production of two quarks by a gluon and the second one stands for the emission of a real gluon by a quark. It is easy to see that the square of expression (3.24) leads to the first term in the square brackets of expression (3.25). It corresponds to diagram 3.11.a. The integral over  $z$  was originally the integral over  $\beta_k$ . The evaluation of the second term in the square brackets of (3.25) follows the same strategy as was used before. I.e. extracting terms

proportional to  $\frac{q^1}{q^4}$  leads to the usual Altarelli-Parisi splitting function convoluted with the Pomeron splitting function derived in the previous section.

We have to give a warning at this place. It is not possible to use expression (3.25) to make realistic computation on three jet events. This can only be done with the help of Monte Carlo simulations. We emphasize that expression (3.25) is only one step on the way to a complete expression of diffractive dissociation cross section.

### 3.3 Higher twist $\frac{1}{q^4}$ :

When we speak of 'higher twist  $\frac{1}{k^4}$ ' or ' $\frac{1}{q^4}$ ', we refer to diagram 3.11 for notation and definition. Having in mind that  $|k^2|$  and  $|q^2|$  are strongly ordered it is obvious that the higher twist contribution  $\frac{1}{k^4}$  is much larger than  $\frac{1}{q^4}$ . We will see that, indeed, in the case of three jet emission we can neglect this contribution, but we have to be careful in the case of the total cross section of diffractive dissociation. The total cross section is evaluated with the help of the evolution equation as explained in section 2, and we cannot exclude this contribution, since it has the same number of leading logs as the higher twist  $\frac{1}{k^4}$  contribution. Nevertheless, we hope that numerical studies will reveal the smallness of this contribution.

Unfortunately we cannot calculate the higher twist  $\frac{1}{q^4}$  contribution with the same accuracy with respect to the ratio  $\frac{\beta_k}{\beta_u}$  as we did deriving the Pomeron splitting functions. We are only able to do this in the Triple Regge Region where  $\beta_u$  is much larger than  $\beta_k$  and  $x$ . This corresponds to the Double Leading log Approximation (DLA).

First of all we reduce expression (3.25) to the DLA region by taking the leading singularity of the Pomeron splitting function:

$$\begin{aligned} \left. \frac{\beta_u d\sigma}{d\beta_u dt} \right|_{t=0} \Big|_{\beta_u \gg x} &= \sum_F \frac{4\pi^2 \alpha_{em} e_F^2}{|Q^2|} \int_{|\bar{Q}_0^2|}^{|\bar{Q}^2|} \frac{d|k^2|}{k^4} \frac{\alpha_s^2}{16} \int_{|k^2|}^{|\bar{Q}^2|} \frac{d|q^2|}{|q^2|} \frac{\alpha_s}{4\pi} \cdot \\ &\cdot \frac{8N^2}{N^2-1} \int_{\frac{x}{\beta_u}}^1 dz \Phi_G^F(z) \left( 4C_F \int_{|\bar{Q}_0^2|}^{|\bar{Q}^2|} \frac{d|l_t^2|}{|l_t^2|} \frac{\alpha_s}{4\pi} \right)^2. \end{aligned} \quad (3.27)$$

In the next step we add the higher twist  $\frac{1}{q^4}$  contribution which is proportional to  $\frac{k^2}{q^2}$  (for details see appendix):

$$\begin{aligned} \left. \frac{\beta_u d\sigma}{d\beta_u dt} \right|_{t=0} \Big|_{\beta_u \gg x} &= \sum_F \frac{4\pi^2 \alpha_{em} e_F^2}{|Q^2|} \int_{|\bar{Q}_0^2|}^{|\bar{Q}^2|} \frac{d|k^2|}{k^4} \frac{\alpha_s^2}{16} \int_{\frac{x}{\beta_u}}^1 dz \int_{\frac{|k^2|}{1-z}}^{|\bar{Q}^2|} \frac{d|q^2|}{|q^2|} \frac{\alpha_s}{4\pi} \cdot \\ &\cdot \frac{8N^2}{N^2-1} \left[ z^2 + (1-z)^2 + 3z(1-z)(2z-1) \frac{k^2}{q^2} \right] \left( 4C_F \int_{|\bar{Q}_0^2|}^{|\bar{Q}^2|} \frac{d|l_t^2|}{|l_t^2|} \frac{\alpha_s}{4\pi} \right)^2. \end{aligned} \quad (3.28)$$

The first term in square brackets is the explicit representation of the Altarelli-Parisi splitting function  $\Phi_G^F$ . The second term is the modified splitting function which we introduced in section 2 as  $\bar{\Phi}_G^F$ .

If we look at the splitting function  $3z(1-z)(2z-1)$  we see that its integral taken over the interval from 0 to 1 is zero. This indicates that the coefficient in front of the higher twist  $\frac{1}{q^4}$  contribution is small. Although this estimation cannot give the final answer we have good hope that the higher twist contribution  $\frac{1}{q^4}$  turns out to be numerical negligible.

## 4 Generalization to multi jet production and the proton structure function:

Since we are interested in the total cross section of diffractive dissociation, we have to go beyond the three jet production and take into account the emission of an arbitrary number of jets. Moreover, we have to improve our simple model of the Pomeron just being made up of a pair of gluons in the colour singlet state. The second point just mentioned is quickly done, for we only need to introduce the gluon structure function  $D_p^G$  by making the substitution:

$$4C_F \int_{|Q_0^2|}^{|k^2|} \frac{d|l_t^2|}{|l_t^2|} \frac{\alpha_s}{4\pi} \rightarrow \beta_u D_p^G(\beta_u, |k^2|, |Q_0^2|) . \quad (4.1)$$

As far as the production of jets is concerned the answer is quite simple if only the higher twist  $\frac{1}{k^4}$  contribution dominates. Then we can proceed as in subsection 3.2 and each extra emitted gluon or quark results in a logarithmic integration over its transverse momentum or virtuality together with the corresponding Altarelli-Parisi splitting function. Taking eq. (3.25) we just have to substitute the Altarelli-Parisi splitting function by the parton density function, for example  $\Phi_F^F$  by  $D_F^F$ . This procedure yields

$$\begin{aligned} \left. \frac{\beta_u d\sigma}{d\beta_u dt} \right|_{t=0} &= \sum_F \frac{4\pi^2 \alpha_{em} e_F^2}{|Q^2|} \int_{\frac{x}{\beta_u}}^1 \frac{dz}{z} \frac{x}{\beta_u} \int_{\frac{|Q_0^2|}{1-z}}^{|Q^2|} \frac{d|k^2|}{k^4} \frac{\alpha_s^2}{16} \cdot \\ &\cdot \left[ \Phi_P^G(z) D_G^F \left( \frac{x}{z\beta_u}, |Q^2|, |k^2| \right) + \Phi_P^F(z) D_F^F \left( \frac{x}{\beta_u z}, |Q^2|, |k^2| \right) \right] \cdot \\ &\cdot \left[ \beta_u D_p^G(\beta_u, |k^2|, |Q_0^2|) \right] . \end{aligned} \quad (4.2)$$

The generalization of the next to leading order is much more complicated and to solve this problem it needs more effort in future time. What we can say is that we can substitute the contribution due to a simple quark loop at the top of the diagram 3.11.a, which is equivalent to a  $\delta$ -function in the variable  $z$ , by the parton density function  $D_F^F$ . Emission

below the quark loop is of that type which was investigated in ref. [?, ?]. It turns out to be a small contribution (see also subsection 2.4.). All that we know about the next to leading contribution was derived in the Triple Regge Region. Nevertheless, we included this contribution in eq. (3.32) (see eq. (2.24) at the beginning of subsection 2.4.). Anyway, we believe that the influence of the next to leading term is small. If not, this term gives, at least, a rough impression how the correction looks like.

## 5 Conclusions:

We have discussed the results of the paper in section 2.4, so we do not need to do this again. However we would like to repeat once more the main physical outcome from our calculations.

1. We claim that AGK cutting rules are violated in deep inelastic scattering as soon as quarks are involved. This fact we conclude from comparison with the paper of Mueller and Qui [?]. In our calculations we see that contributions which are necessary to restore the AGK cutting rules are suppressed by a factor of the type  $x_B \ln(1/x_B)$ . We have not understood the physical meaning and the general origin of this important result and consider this problem as one of high priority for the future. We propose to calculate all cuts in deep inelastic scattering in order to clear up what the real source of the AGK cutting rule violation is, and what replaces the AGK cutting rule in deep inelastic processes.
2. We started to study theoretically the hypothesis of the Pomeron structure function and found that we could discuss the process of diffractive dissociation introducing such a function only in a limited kinematical region and as a very rough estimation. We cannot support the idea that the Pomeron could be viewed as a real particle.
3. We got a formula for the diffractive dissociation that could be used for a Monte Carlo simulation. There we introduced two new functions (Pomeron splitting functions)

$$\begin{aligned}\Phi_P^F(z) &= \frac{8}{N} z^2(1-z) \\ \Phi_P^G(z) &= \frac{8N^2}{N^2-1} z(1-z)^2 \left(2 + \frac{1}{z}\right)^2\end{aligned}\tag{5.1}$$

which allow to use our formula in the region

$$0 \leq \frac{M_X^2}{s} \ll s .\tag{5.2}$$

We hope that this will help to study diffractive dissociation at HERA.

**Acknowledgements:** We would like to thank J.Bartels who initiated one of us (M.W.) to work on this subject as well as N.N.Nikolaev and M.G.Ryskin for fruitful discussions. One of us (E.L.) is also grateful to the DESY and FNAL Theory Divisions for their kind hospitality.

## Appendix:

### A

In this appendix we would like to come back to the discussion of the AGK-cutting rules and calculate the integral (2.31) in order to establish the correspondance between our calculation and the calculation of Mueller and Qui [?] for the shadowing correction to the usual evolution equation. To reconstruct all normalization factors we prefer to use the analysis which was developed in [?]. There was discussed what we actually need here, the interaction of two Pomerons with a nucleus, since it is the same model on which the calculations in [?] are based.

The function  $M(\vec{u}, \nu)$  can be regarded as the cross section of a process where some probe is scattered off the nucleus with the momentum transfer  $\vec{u}$ . The energy transfer  $u_0 = \nu$  is small compared to the target mass. If  $U(\vec{x})$  is the effective 'potential' of the probe-nucleus interaction the cross section is given by the familiar formula

$$M(\vec{u}, \nu) = \sum_f \left| \langle f | \int d^3 \vec{x} U(\vec{x}) e^{i(\vec{u}, \vec{x})} | i \rangle \right|^2 \delta(E_f + \nu - E_i) \quad (\text{A.1})$$

where  $E_{i,f}$  are the energies of the initial and final state. In our model  $U(\vec{x})$  is the sum of terms describing the interaction with the individual constituents of the nucleus which are located at  $\vec{x}_j$ :

$$U(\vec{x}) = \sum_j^A V(\vec{x} - \vec{x}_j) \quad (\text{A.2})$$

Using the closure property of the final state

$$\sum_f |f\rangle \langle f| = 1 \quad (\text{A.3})$$

we find

$$\int d\nu M(\vec{u}, \nu) = v^2(\vec{u}) \left[ A + \sum_{m \neq n} \langle i | e^{i(\vec{u}, \vec{x}_m - \vec{x}_n)} | i \rangle \right] \quad (\text{A.4})$$

where  $v(\vec{u})$  is the Fourier transform of  $V(\vec{x})$ . We repeat these arguments for the sake of completeness. The only important remark that we would like to make is the fact that  $\nu$  is proportional to  $\frac{\alpha_u}{2}$  which follows from the definition of  $\alpha_u$ . It should be stressed that we used the nonrelativistic normalization of the wave function of the nucleon inside the nucleus which gave us the eqs. (A.3) and (A.5) together with the  $\delta$ -function in eq. (A.1). Such a normalization allows to simplify the calculation by utilizing one of the widely spread approximations for the nucleus wave function, i.e. the gas approximation (see below).

We are able to rewrite expression (A.4) through the nuclear ground state function  $\varphi(\vec{x}_1, \dots, \vec{x}_A)$ , namely

$$\langle i | e^{i(\vec{u}, \vec{x}_m - \vec{x}_n)} | i \rangle = \int \prod_j d^3 \vec{x} |\varphi(\vec{x}_1, \dots, \vec{x}_A)|^2 e^{i(\vec{u}, \vec{x}_m - \vec{x}_n)} \quad (\text{A.5})$$

In the nuclear-gas approximation

$$|\varphi(\vec{x}_1, \dots, \vec{x}_A)|^2 = \prod_j \rho(\vec{x}_j) \quad (\text{A.6})$$

one gets

$$\sum_{m \neq n} \langle i | e^{i(\vec{u}, \vec{x}_m - \vec{x}_n)} | i \rangle = A(A-1) |F(\vec{u}^2)|^2 \quad (\text{A.7})$$

where

$$F(\vec{u}^2) = \int d^3 \vec{u} \rho(\vec{x}) e^{i(\vec{u}, \vec{x})} . \quad (\text{A.8})$$

So we rewrite the integral in eq. (2.31) (section 2) in the following way

$$\begin{aligned} \int d\vec{u}_t^2 M(\vec{u}_t^2) &= 2 A(A-1) \int d\vec{u}_t^2 |F(\vec{u}_t^2)|^2 \\ &= 2 A(A-1) \int \frac{d^2 \vec{u}_t}{\pi} |F(\vec{u}_t^2)|^2 \\ &= 8\pi A(A-1) \int dz_1 dz_2 d^2 \vec{r}_t \rho(z_1, \vec{r}_t) \rho(z_2, \vec{r}_t) \end{aligned} \quad (\text{A.9})$$

From (A.9) we get in the case of a black nucleus

$$\begin{aligned} \int d\vec{u}_t^2 M(\vec{u}_t^2) &= A^2 \frac{9}{R_A^2} \\ &= A 12\pi R_A \rho \end{aligned} \quad (\text{A.10})$$

where  $\rho$  is the nucleon density in a nucleus.

We discuss this normalization in details only to compare with the calculation of Mueller and Qui [?] and to drive to a definite conclusion on the AGK-cutting rules. Using eq. (A.10) we get that result which has been discussed under point 3 of subsection 2.4.

## B.1

In this part of the appendix we present some more details about the calculation in subsection 3.1 starting with fig. 3.3. By summing the two diagrams in fig. 3.1 we will show in an explicit way that the polarization vector  $p^\rho$  can be substituted by  $-\frac{l_t^\rho}{\beta_l + \beta_u}$ :

$$\bar{u}(k+Q) \gamma_t^\mu \frac{\hat{k}}{k^2} \hat{p} v(k-l-u) + \bar{u}(k+Q) \hat{p} \frac{\hat{k} + \hat{Q} - \hat{l} - \hat{u}}{(k+Q-l-u)^2} \gamma_t^\mu v(k-l-u) . \quad (\text{B.1.1})$$

The denominator  $(k+Q-l-u)^2$  is equal to  $-(\beta_l + \beta_u)s$ . Each  $s$  in the denominator has to be compensated by some  $s$  in the numerator. This can be achieved only by taking the leading contribution of the expression  $\bar{u}(k+Q) \hat{p} (\hat{k} + \hat{Q} - \hat{l} - \hat{u})$  which is  $s \bar{u}(k+Q)$ . Furthermore, we can change  $\hat{p} v(k-l-u)$  into  $\frac{\hat{k} - \hat{l}}{\beta_l + \beta_u} v(k-l-u)$  after the multiplication and the division by  $\beta_l + \beta_u$ . We then see the cancellation of the leading terms in (B.1.1) which results in:

$$\bar{u}(k+Q) \gamma_t^\mu \frac{\hat{k}}{k^2} \left( -\frac{\hat{l}_t}{\beta_l + \beta_u} \right) v(k-l-u) . \quad (\text{B.1.2})$$

This is exactly what we wanted to proof.

We proceed with equation (3.9) of subsection 3.1 and recall the first expression:

$$- \bar{u}(k+Q) \gamma_t^\mu \frac{\hat{k}}{k^2} \frac{\hat{l}_t}{\beta_l + \beta_u} (\hat{k} - \hat{l} - \hat{u}) \hat{p} v(k-u) \frac{\pi}{\alpha_k s} . \quad (\text{B.1.3})$$

In the first step we extract all terms of the order  $l_t^2$  which are the leading terms. The terms of the order  $l_t^1$  cancel out. It is enough to expand each of the factors  $\hat{k} - \hat{l} - \hat{u}$  and  $\frac{1}{\beta_l + \beta_u}$  to the first order in  $l_t$ . We should remind here that  $\beta_l$  depends on  $l_t$ :

$$\beta_l = \frac{l_t^2 - 2(l_t, k_t)}{\alpha_k s} . \quad (\text{B.1.4})$$

In the expression  $(\hat{k} - \hat{l} - \hat{u}) \hat{p}$   $\beta_l$  does not contribute, since  $\beta_l \hat{p} \hat{p}$  is equal to zero. The factor  $\frac{1}{\beta_l + \beta_u}$  leads to  $\frac{1}{\beta_u} \frac{2(l_t, k_t)}{\beta_u \alpha_k s}$ . So we have:

$$- \bar{u}(k+Q) \gamma_t^\mu \frac{\hat{k}}{k^2} \frac{\hat{l}_t}{\beta_u} \left[ \frac{2(l_t, k_t)}{\beta_u \alpha_k s} (\hat{k} - \hat{u}) - \hat{l}_t \right] \hat{p} v(k-u) \frac{\pi}{\alpha_k s} . \quad (\text{B.1.5})$$

Integration over the azimuth angle of  $l_t$  yields:

$$- \bar{u}(k+Q) \gamma_t^\mu \frac{\hat{k}}{k^2} \left[ \frac{\hat{k}_t}{\beta_u^2 \alpha_k s} (\hat{k} - \hat{u}) \hat{p} - \frac{\hat{p}}{\beta_u} \right] v(k-u) \frac{\pi l_t^2}{\alpha_k s} . \quad (\text{B.1.6})$$

Now and for further transformations we frequently use the following identity:

$$\bar{u}(k+Q) \gamma_t^\mu \hat{Q}' \approx 0 . \quad (\text{B.1.7})$$

This is easily proved by taking the square of the expression (B.1.7):

$$Sp\{\gamma_t^\mu (\hat{k} + \hat{Q}) \gamma_{t\mu} \hat{Q}' \dots\} \approx 0 . \quad (\text{B.1.8})$$

Since  $\beta_k$  is equal to  $x$  we find that  $\gamma_t^\mu (\hat{k} + \hat{Q}) \gamma_{t\mu}$  approximately coincides with  $\hat{Q}'$  where we neglect terms proportional to  $\frac{k_t^2}{s}$ . Remembering the fact that  $u = \beta_u p$  we can write (B.1.6) as:

$$- \frac{\pi l_t^2}{\beta_u k^2} \bar{u}(k+Q) \gamma_t^\mu \left[ \frac{\beta_k \hat{p} \hat{k}_t \hat{k} \hat{p} + k_t^2 \hat{k} \hat{p}}{\beta_u \alpha_k^2 s^2} - \frac{\hat{k} \hat{p}}{\alpha_k s} \right] v(k-u) . \quad (\text{B.1.9})$$

The next simplification comes from the identity  $\hat{k} \hat{p} v(k-u) = \alpha_k s v(k-u)$  where, again, we make use of the relation  $u = \beta_u p$  and  $p^2 = 0$ . From table 3.3 we get  $\beta_u \alpha_k s = \frac{k_t^2}{1-z}$  with  $z = \frac{\beta_k}{\beta_u}$ , and eq. (B.1.9) can be transformed into:

$$- \frac{\pi l_t^2}{\beta_u k^2} \bar{u}(k+Q) \gamma_t^\mu \left[ z \frac{\hat{p} \hat{k}_t}{\alpha_k s} - z \right] v(k-u) . \quad (\text{B.1.10})$$

For further reduction we use the following chain of relations:  $\hat{p} \hat{k}_t v(k-u) = \hat{p} (\hat{k} - \alpha_k \hat{Q}') v(k-u) = -\hat{p} \alpha_k \hat{Q}' v(k-u) = (-\alpha_k s + \alpha_k \hat{Q}' \hat{p}) v(k-u)$ , and with the help of eq. (B.1.7) we finally find:

$$\frac{\pi l_t^2}{\beta_u k^2} 2z \bar{u}(k+Q) \gamma_t^\mu v(k-u) . \quad (\text{B.1.11})$$

Next, we evaluate the second expression of eq. (3.9):

$$\bar{u}(k+Q) \hat{p} (\hat{k} + \hat{Q} + \hat{l}) \gamma_{t\mu} \frac{\hat{k} + \hat{l}}{(k+l)^2} \frac{\hat{l}_t}{\beta_l + \beta_u} v(u-k) \frac{\pi}{s} . \quad (\text{B.1.12})$$

The  $s$  in the denominator can only be compensated by the leading term of  $\bar{u}(k+Q) \hat{p} (\hat{k} + \hat{Q} + \hat{l})$  which is  $s \bar{u}(k+Q)$ .  $\beta_l$  is zero in this case. The expansion of the propagator gives

$$\frac{1}{(k+l)^2} \approx \frac{1}{k^2} - \frac{2(l_t, k_t)}{k^4} , \quad (\text{B.1.13})$$

Extracting the terms of second order in  $l_t$  from the total expression (B.1.12) leads to:

$$\frac{\pi}{\beta_u k^2} \bar{u}(k+Q) \gamma_{t_\mu} \left( -\frac{\hat{k} \hat{l}_t 2(l_t, k_t)}{k^2} + l_t^2 \right) v(u-k). \quad (\text{B.1.14})$$

Integration over the azimuth angle of  $l_t$  yields:

$$\frac{\pi l_t^2}{\beta_u k^2} \bar{u}(k+Q) \gamma_{t_\mu} \left( -\frac{\hat{k} \hat{k}_t}{k^2} + 1 \right) v(u-k). \quad (\text{B.1.15})$$

Using the eq. (B.1.7) and the relation  $k^2 = \frac{k^2}{1-z}$  finally results in the same expression as in eq. (B.1.10). This means that the sum of all diagrams in fig. 3.1, i.e. the final answer of this subsection, is equal to expression (B.1.11) multiplied by two:

$$\frac{\pi l_t^2}{\beta_u k^2} 4z \bar{u}(k+Q) \gamma_t^\mu v(k-u). \quad (\text{B.1.16})$$

## B.2

In this subsection of the appendix we come back to the calculation of the diagrams in fig. 3.7 and 3.8. These diagrams describe the process of diffractive dissociation including the emission of one gluon.

We start with diagram 3.7.a and take out the right gluon vertex:

$$\begin{aligned} & \Gamma_{\mu\nu\rho}(l+u-k, -l, k-u) \\ &= g_{\mu\nu}(-2l-u+k)_\rho + g_{\nu\rho}(k-u+l)_\mu + g_{\rho\mu}(l+2u-2k)_\nu. \end{aligned} \quad (\text{B.2.1})$$

The gluons to the left with the momentum  $l+u-k$  and to the right with the momentum  $u-k$  are on mass-shell, so that we can use the polarization vector  $\epsilon^\mu(l+u-k)$  and  $\epsilon^\rho(u-k)$  for real gluons. From below we have  $p^\nu$  as polarization vector.

$$\begin{aligned} & \epsilon^\mu(l+u-k) \epsilon^\rho(u-k) \Gamma_{\mu\nu\rho} p^\nu \\ &= (p, \epsilon(l+u-k)) (-2l, \epsilon(u-k)) + (2l, \epsilon(l+u-k)) (p, \epsilon(u-k)) \\ &- \alpha_{ks} (\epsilon(l+u-k), \epsilon(u-k)). \end{aligned} \quad (\text{B.2.2})$$

This expression yields:

$$\begin{aligned} & 2 \frac{(l_t - k_t, \epsilon_t(l+u-k))}{\beta_l + \beta_u - \beta_k} (l_t, \epsilon_t(u-k)) + 2 (l_t, \epsilon_t(l+u-k)) \frac{(k_t, \epsilon_t(u-k))}{\beta_u - \beta_k} \\ &- \alpha_{ks} (\epsilon_t(l+u-k), \epsilon_t(u-k)). \end{aligned} \quad (\text{B.2.3})$$

Next, we take the left gluon vertex:

$$\begin{aligned} & \Gamma_{\mu\nu\rho}(-l-u+k, -k, l+u) \\ &= g_{\mu\nu}(-2k+l+u)_\rho + g_{\nu\rho}(l+u+k)_\mu + g_{\rho\mu}(-2l-2u+k)_\nu. \end{aligned} \quad (\text{B.2.4})$$

We will use the polarization vector  $\epsilon^\nu(k)$  even for an off mass-shell gluon. This is possible, since  $Q^\nu$  applied to the upper quark loop does not contribute, at least not at the desired order. From below we now have  $-\frac{l_t^p}{\beta_l+\beta_u}$ .

$$\begin{aligned} & \epsilon^\nu(k) \epsilon^\mu(l+u-k) \Gamma_{\mu\nu\rho} \left( -\frac{l_t^p}{\beta_l+\beta_u} \right) \\ &= (\epsilon(k), \epsilon(l+u-k)) \frac{2(l_t, k_t) - l_t^2}{\beta_l+\beta_u} - 2 \frac{(l_t, \epsilon(k))}{\beta_l+\beta_u} (l+u, \epsilon(l+u-k)) \\ &+ 2 \frac{(l_t, \epsilon(l+u-k))}{\beta_l+\beta_u} (l+u, \epsilon(k)). \end{aligned} \quad (\text{B.2.5})$$

This expression is evaluated to be:

$$\begin{aligned} & (\epsilon_t(k), \epsilon_t(l+u-k)) \frac{2(l_t, k_t) - l_t^2}{\beta_l+\beta_u} - 2(l_t, \epsilon_t(k)) \frac{(l_t - k_t, \epsilon_t(l+u-k))}{\beta_l+\beta_u - \beta_k} \\ &- 2 \frac{(l_t, \epsilon_t(l+u-k))}{\beta_k} (k_t, \epsilon(k)). \end{aligned} \quad (\text{B.2.6})$$

Next, we have to multiply (B.2.6) and (B.2.3) and sum over the polarization of the gluon with momentum  $l+u-k$ :

$$\begin{aligned} & 4 \frac{(l_t - k_t, \epsilon_t(k))}{\beta_l+\beta_u - \beta_k} (l_t, \epsilon_t(u-k)) \frac{(l_t, k_t) - \frac{1}{2}l_t^2}{\beta_l+\beta_u} + 4(l_t, \epsilon_t(k)) \frac{(l_t - k_t)^2 (l_t, \epsilon_t(u-k))}{(\beta_l+\beta_u - \beta_k)^2} \\ &- 4 \frac{(l_t, l_t - k_t)}{\beta_l+\beta_u - \beta_k} \frac{(k_t, \epsilon_t(k))}{\beta_k} (l_t, \epsilon_t(u-k)) + 4(l_t, \epsilon_t(k)) \frac{(k_t, \epsilon_t(u-k))}{\beta_u - \beta_k} \frac{(l_t, k_t) - \frac{1}{2}l_t^2}{\beta_l+\beta_u} \\ &+ 4(l_t, \epsilon_t(k)) \frac{(l_t, l_t - k_t)}{\beta_l+\beta_u - \beta_k} \frac{(k_t, \epsilon_t(u-k))}{\beta_u - \beta_k} - 4l_t^2 \frac{(k_t, \epsilon_t(k))}{\beta_k} \frac{(k_t, \epsilon_t(u-k))}{\beta_u - \beta_k} \quad (\text{B.2.7}) \\ &- 2\alpha_k s (\epsilon_t(k), \epsilon_t(u-k)) \frac{(l_t, k_t) - \frac{1}{2}l_t^2}{\beta_l+\beta_u} - 2\alpha_k s (l_t, \epsilon_t(k)) \frac{(l_t - k_t, \epsilon_t(u-k))}{\beta_l+\beta_u - \beta_k} \\ &+ 2\alpha_k s \frac{(l_t, \epsilon_t(u-k))}{\beta_k} (k_t, \epsilon_t(k)). \end{aligned}$$

From this expression we would like to extract the second order in  $l_t$ . While we do this we have to take into account that  $\beta_l$  depends on  $l_t$ :

$$\begin{aligned} \frac{1}{\beta_l+\beta_u} &\approx \frac{1}{\beta_u} + \frac{2(l_t, k_t)}{\beta_u^2 \alpha_k s}; \\ \frac{1}{\beta_l+\beta_u - \beta_k} &\approx \frac{1}{\beta_u - \beta_k} + \frac{2(l_t, k_t)}{(\beta_u - \beta_k)^2 \alpha_k s}. \end{aligned} \quad (\text{B.2.8})$$

So we get:

$$\begin{aligned}
& - 4 \frac{(k_t, \epsilon_t(k))}{\beta_u - \beta_k} (l_t, \epsilon_t(u - k)) \frac{(l_t, k_t)}{\beta_u} + 4 (l_t, \epsilon_t(k)) \frac{k_t^2}{(\beta_u - \beta_k)^2} (l_t, \epsilon_t(u - k)) \\
& + 4 \frac{(l_t, k_t)}{\beta_u - \beta_k} \frac{(k_t, \epsilon_t(k))}{\beta_k} (l_t, \epsilon_t(u - k)) + 4 (l_t, \epsilon_t(k)) \frac{(k_t, \epsilon_t(u - k))}{\beta_u - \beta_k} \frac{(l_t, k_t)}{\beta_u} \\
& - 4 (l_t, \epsilon_t(k)) \frac{(l_t, k_t)}{\beta_u - \beta_k} \frac{(k_t, \epsilon_t(u - k))}{\beta_u - \beta_k} - 4 l_t^2 \frac{(k_t, \epsilon_t(k))}{\beta_k} \frac{(k_t, \epsilon_t(u - k))}{\beta_u - \beta_k} \quad (\text{B.2.9}) \\
& + \alpha_k s (\epsilon_t(k), \epsilon_t(u - k)) \frac{l_t^2}{\beta_u} - 4 (\epsilon_t(k), \epsilon_t(u - k)) \frac{(l_t, k_t)^2}{\beta_u^2} \\
& - 2 \alpha_k s (l_t, \epsilon_t(k)) \frac{(l_t, \epsilon_t(u - k))}{\beta_u - \beta_k} + 4 (l_t, \epsilon_t(k)) \frac{(k_t, \epsilon_t(u - k))}{\beta_u - \beta_k} \frac{(l_t, k_t)}{\beta_u - \beta_k} .
\end{aligned}$$

Integration over the azimuth angle of  $l_t$  yields:

$$\begin{aligned}
& - 2 \frac{(k_t, \epsilon_t(k))}{\beta_k} \frac{(k_t, \epsilon_t(u - k))}{\beta_u - \beta_k} l_t^2 + 2 (\epsilon_t(k), \epsilon_t(u - k)) \frac{k_t^2}{(\beta_u - \beta_k)^2} l_t^2 \\
& + \alpha_k s (\epsilon_t(k), \epsilon_t(u - k)) \frac{l_t^2}{\beta_u} - 2 (\epsilon_t(k), \epsilon_t(u - k)) \frac{k_t^2}{\beta_u} l_t^2 \quad (\text{B.2.10}) \\
& - \alpha_k s (\epsilon_t(k), \epsilon_t(u - k)) \frac{l_t^2}{\beta_u - \beta_k} .
\end{aligned}$$

In the following equations we would like to include the residue of the  $\beta_t$ -integration together with the corresponding  $\pi$  and the factor  $\frac{1}{k^2}$  originating from the propagator. All this leads to an extra factor

$$\frac{\pi}{\alpha_k s k^2} . \quad (\text{B.2.11})$$

With  $z = \frac{\beta_k}{\beta_u}$  and  $\beta_u \alpha_k s = k^2$ . we reduce the eq. (B.2.10):

$$\frac{\pi l_t^2}{\beta_u k^2} \left\{ - \frac{2}{z(1-z)} \frac{(k_t, \epsilon_t(k))(k_t, \epsilon_t(u - k))}{k^2} + z \frac{3-2z}{1-z} (\epsilon_t(k), \epsilon_t(u - k)) \right\} . \quad (\text{B.2.12})$$

The next diagrams which we will calculate are those in fig. 3.7.c and 3.7.d. The right gluon vertex is the same as in fig. 3.7.a. Instead of the left gluon vertex we now have:

$$- \frac{(k_t, \epsilon_t(k)) (2p, \epsilon_t(l + u - k))}{\beta_k \alpha_k s} l_t^2 = 2 \frac{(l_t - k_t, \epsilon_t(l + u - k))}{(l_t - k_t)^2} l_t^2 \frac{(k_t, \epsilon_t(k))}{\beta_k} . \quad (\text{B.2.13})$$

The  $\alpha_k s$  comes from the propagator at the bottom line. In order to make expression (B.2.13) comparable with the diagram 3.7.a we multiplied by  $l_t^2$ . Later on we will divide all contributions by  $l_t^4$  which corresponds to the the two propagators with momentum  $l + u$  and  $l$  in

diagram 3.7.a. In the further procedure we multiply expression (B.2.13) by (B.2.3) and sum over the polarization as before. Since expression (B.2.13) is already of second order in  $l_t$  we only need to take the third term in eq. (B.2.3). The result is:

$$2 \frac{(k_t \epsilon_t(k))}{\beta_k} \alpha_{ks} l_t^2 \frac{(k_t, \epsilon_t(u-k))}{k_t^2}. \quad (\text{B.2.14})$$

After multiplication by the factor (B.2.11) we see that this result cancels the first term in expression (B.2.12). Indeed, taking into account diagram 3.7.d the colour coefficient adds up to give the same as in diagram 3.7.a. So we are left with

$$\frac{\pi l_t^2}{\beta_u k^2} z \frac{3-2z}{1-z} (\epsilon_t(k), \epsilon_t(u-k)). \quad (\text{B.2.15})$$

The last diagram in the first group is the one in fig. 3.7.b. We have already discussed in subsection 3.2 that the quark pair at the top of the diagram acts as a classical current with regard to the soft gluon with momentum  $l+u-k$ . One conclusion was that the  $\beta$ -component equals zero. So we have:

$$\beta_l + \beta_u = \beta_k. \quad (\text{B.2.16})$$

The gluon vertex is the same as in expression (B.2.1), but from the top we now have  $\frac{Q'^{\mu}}{(p, Q')}$  and from the bottom  $-\frac{l_t^{\nu}}{\beta_l}$ :

$$\frac{Q'^{\mu}}{(p, Q')} \left( -\frac{l_t^{\nu}}{\beta_l} \right) \Gamma_{\mu\nu\rho}(l+u-k, -l, k-u) \epsilon^{\rho}(u-k) = -(\beta_k - \beta_u + \beta_l) \frac{(l_t, \epsilon_t(u-k))}{\beta_l}. \quad (\text{B.2.17})$$

Taking into account (B.2.16) we find the simple result:

$$-2(l_t, \epsilon_t(u-k)). \quad (\text{B.2.18})$$

The left lower t-channel gluon which carries the momentum  $l+u$  gives a contribution of the type:

$$-\frac{(l_t, \epsilon_t(k))}{\beta_l + \beta_u} = -\frac{(l_t, \epsilon_t(k))}{\beta_k}. \quad (\text{B.2.19})$$

The denominator  $(l+u-k)^2$  corresponding to the right upper t-channel gluon simply yields  $(k_t - l_t)^2$ . Together with (B.2.18) and (B.2.19) the final integration over the azimuth angle of  $l_t$  leads to

$$\frac{l_t^2}{\beta_u k^2} \frac{1}{z(1-z)} (\epsilon_t(k), \epsilon_t(u-k)). \quad (\text{B.2.20})$$

The residue of the  $\beta_l$ -integration was canceled out by the emission vertex of the soft gluon with momentum  $l+u-k$ <sup>16</sup>. We only keep the  $\pi$  which has not been taken into account

---

<sup>16</sup>typical for classical current emission

yet. Finally we have to be aware of the opposite sign with respect to diagram 3.7.a. which is due to colour.

We can now write down the final expression for the total sum of all diagrams in fig. 3.7:

$$\begin{aligned} & \frac{\pi l_t^2}{\beta_u k^2} \left( z \frac{3-2z}{1-z} - \frac{1}{z(1-z)} \right) (\epsilon_t(k), \epsilon_t(u-k)) \\ &= \frac{\pi l_t^2}{\beta_u k^2} (1-z) \left( 2 + \frac{1}{z} \right) (\epsilon_t(k), \epsilon_t(u-k)) . \end{aligned} \quad (\text{B.2.21})$$

Our next task is the calculation of the diagrams in fig. 3.8. The gluon vertex in diagram 3.8.a is:

$$\begin{aligned} & \Gamma_{\mu\nu\rho}(-l-k, l+u, k-u) \\ &= g_{\mu\nu}(-2l-u+k)_\rho + g_{\nu\rho}(k-u+l)_\mu + g_{\rho\mu}(l+2u-2k)_\nu . \end{aligned} \quad (\text{B.2.22})$$

The procedure is similar to that before in the case of diagram 3.7.a. For the gluon with momentum  $l+k$  we use the polarization vector  $\epsilon^\mu(l+k)$ . From below we have as usual  $-\frac{l_t^\nu}{\beta_l+\beta_u}$ , and we apply the polarization vector  $\epsilon^\rho(u-k)$  which corresponds to the emitted real gluon.

$$\begin{aligned} & \epsilon^\mu(l+k) \left( -\frac{l_t^\nu}{\beta_l+\beta_u} \right) \Gamma_{\mu\nu\rho} \epsilon^\rho(u-k) \\ &= -\frac{(l_t, \epsilon_t(l+k))}{\beta_l+\beta_u} 2(l+u, \epsilon(u-k)) + 2(l+u, \epsilon(l+k)) \frac{(l_t, \epsilon_t(u-k))}{\beta_l+\beta_u} \\ &+ (\epsilon(l+k), \epsilon(u-k)) \frac{l_t^2 + 2(l_t, k_t)}{\beta_l+\beta_u} . \end{aligned} \quad (\text{B.2.23})$$

Further evaluation gives

$$\begin{aligned} & -2(l_t, \epsilon_t(l+k)) \frac{k_t, \epsilon_t(u-k)}{\beta_u-\beta_k} - 2(l_t, k_t) \frac{(l_t+k_t, \epsilon_t(l+k))}{\beta_l+\beta_k} \\ &+ (\epsilon_t(l+k), \epsilon_t(u-k)) \frac{l_t^2 + 2(l_t, k_t)}{\beta_l+\beta_u} . \end{aligned} \quad (\text{B.2.24})$$

In all diagrams of fig. 3.8 we can set  $\beta_l$  equal to zero. Instead of  $\frac{1}{\beta_l+\beta_u}$  we now have to expand the propagator  $l+k$ :

$$\frac{1}{(l+k)^2} = \frac{1}{l_t^2 + 2(l_t, k_t) + k^2} \approx \frac{1}{k^2} - \frac{2(l_t, k_t)}{k^4} . \quad (\text{B.2.25})$$

After combining this equation with expression (B.2.24) and extracting all terms of second order in  $l_t$  we get:

$$\begin{aligned}
& 2 \frac{(l_t, \epsilon_t(l+k)) 2(l_t, k_t) (k_t, \epsilon_t(u-k))}{k^4} - 2 \frac{(l_t, \epsilon_t(u-k)) (l_t, \epsilon_t(l+k))}{k^2} \\
& + 2 \frac{(l_t, \epsilon_t(u-k)) 2(l_t, k_t) (k_t, \epsilon_t(l+k))}{k^4} + \frac{(\epsilon_t(l+k), \epsilon_t(u-k))}{\beta_u k^2} l_t^2 \\
& - 2 \frac{(\epsilon_t(l+k), \epsilon_t(u-k)) 2(l_t, k_t)^2}{k^4} .
\end{aligned} \tag{B.2.26}$$

We still have to integrate over the azimuth angle of  $l_t$  which results in:

$$\frac{\pi l_t^2}{\beta_u k^2} \left\{ \frac{2}{z(1-z)} \frac{(k_t, \epsilon_t(l+k)) (k_t, \epsilon_t(u-k))}{k^2} - (1-z) \left( 2 + \frac{1}{z} \right) (\epsilon_t(l+k), \epsilon_t(u-k)) \right\} . \tag{B.2.27}$$

where we included a  $\pi$  coming along with the  $\beta_l$ -integration.

We now can already suspect what happens with the first term in eq. (B.2.27), if we add the diagrams 3.8.b and 3.8.c. It is canceled. The proof is quite easy to do. From diagram 3.8.b we have

$$- \frac{(l_t + k_t, \epsilon_t(l+k))}{\beta_l + \beta_k} 2(p, \epsilon(u-k)) \frac{l_t^2}{\alpha_{ks}} \frac{\pi}{(l+k)^2} \tag{B.2.28}$$

which gives:

$$- \frac{\pi l_t^2}{\beta_u k^2} \frac{2}{z(1-z)} \frac{(k_t, \epsilon_t(l+k)) (k_t, \epsilon_t(u-k))}{k^2} . \tag{B.2.29}$$

Diagram 3.8.c yields the same result, but the colour coefficient is different. However, diagram 3.8.b and 3.8.c sum up to give the same coefficient as in diagram 3.8.a. The complete answer for all diagrams in fig. 3.8 is:

$$- \frac{\pi l_t^2}{\beta_u k^2} (1-z) \left( 2 + \frac{1}{z} \right) (\epsilon_t(l+k), \epsilon_t(u-k)) . \tag{B.2.30}$$

Expression (B.2.30) and (B.2.21) can be viewed as identical, although they contain two different vectors  $\epsilon_t(l+k)$  and  $\epsilon_t(k)$ . We introduced these vectors for technical reasons. To get rid of them we have to be aware that in the total amplitude there is a second pair of adjoint vectors  $\epsilon_t^\mu(l+k)$  and  $\epsilon_t^\mu(k)$  which transforms both of them into the projector on the vector component  $\mu$  after summation over the polarization. So we can add up both expressions originating from fig. 3.7 and 3.8 into one:

$$- \frac{\pi l_t^2}{\beta_u k^2} 2 (1-z) \left( 2 + \frac{1}{z} \right) (\epsilon_t(l+k), \epsilon_t(u-k)) . \tag{B.2.31}$$

We should mention that a more careful analysis shows that the sign due to the soft emitted gluon is compensated by the total colour coefficient in fig. 3.8, so that the sum of diagrams in fig. 3.7 and 3.8 have the same sign and do not cancel out.

We conclude this subsection with one example of diagrams (see fig. 3.9) which do not contribute. It is easy to check that this diagram is of third order in  $l_t$ , so beyond the Leading Log Approximation.

### B.3

This subsection deals with the calculation of the higher twist ' $\frac{1}{q^4}$ ' contribution. In order to manage the calculation in this case we have to restrict ourselves to the Double leading Log Approximation. This restriction goes along with the strong ordering of  $\beta_u$  and  $\beta_k$  (Triple Regge Region).

$$\beta_u \gg \beta_k \geq \beta_q = x . \quad (\text{B.3.1})$$

The strategy now is to keep all terms proportional to  $l_t^2$  as usual and in addition to keep only those terms with the leading singularity in  $\beta_k$ .

The diagrams which we need to consider are presented in fig. 3.12. Strictly speaking we already considered these diagrams in fig. 3.7 and 3.8, but we would like to start from the beginning, now, using a slightly different technique.

The main point is to handle the transverse momenta  $k_t$  and  $q_t$  on the same level, although we still assume strong ordering:

$$|q_t| \gg |k_t| . \quad (\text{B.3.2})$$

First of all we concentrate on the gluon vertex of diagram 3.12.a and 3.12.b (see diagram 3.13). What we have to do is to extract from expression (B.2.24) and (B.2.28) the leading singularity in  $\beta_l + \beta_k$ :

$$- 2 \frac{l_t^2}{(l_t + k_t)^2} \left[ \frac{(l_t, \epsilon_t(u - k))}{l_t^2} + \frac{(k_t, \epsilon_t(u - k))}{k_t^2} \right] \frac{(l_t + k_t)^\nu}{\beta_l + \beta_k} . \quad (\text{B.3.3})$$

The above expression already contains the propagator  $\frac{1}{(l_t + k_t)^2}$ . As we will show below it is enough to use the following much simpler expression for further calculation:

$$- 2 \frac{(l_t, \epsilon_t(u - k))}{k_t^2} \frac{(l_t + k_t)^\nu}{\beta_l + \beta_k} . \quad (\text{B.3.4})$$

In order to proof this we expand the first part of expression (B.3.3) (without  $\frac{(l_t + k_t)^\nu}{\beta_l + \beta_k}$ ):

$$- 2 \left[ \frac{(l_t, \epsilon_t(u - k))}{k_t^2} - 2 \frac{(l_t, k_t)(l_t, \epsilon_t(u - k))}{k_t^4} + \frac{l_t^2(k_t, \epsilon_t(u - k))}{k_t^4} \right] . \quad (\text{B.3.5})$$

It is easy to see that the second and third term cancel out after integration over the azimuth angle of  $l_t$ .

$\beta_l$  is fixed in the usual way by taking the imaginary part of the amplitude, i.e. in the case of diagram 3.12.a  $(q - k - l)^2$  is set to zero. It follows that  $\beta_l$  has the value:

$$\beta_l = -\frac{(2l_t, q_t - k_t)}{\alpha_{qs}}. \quad (\text{B.3.6})$$

The factor  $\frac{1}{\beta_l + \beta_k}$  has the expansion:

$$\frac{1}{\beta_l + \beta_k} = \frac{1}{\beta_k} \left( 1 + \frac{(2l_t, q_t - k_t)}{\beta_k \alpha_{qs}} \right). \quad (\text{B.3.7})$$

We can now go on with the evaluation of the fermionic part of the diagram:

$$- 2 \frac{(l_t, \epsilon_t(u - k))}{k_t^2} \bar{u}(q + Q) \gamma_{t\mu} \frac{\hat{q}}{q^2} \frac{\hat{k}_t + \hat{l}_t}{\beta_l + \beta_k} (\hat{q} - \hat{k} - \hat{l}) \hat{p} v(k - q) \frac{\pi}{\alpha_{ks}}. \quad (\text{B.3.8})$$

An important consequence due to DLApproximation is the possibility to neglect  $\alpha_{ks}$ . Using the by now familiar tricks we come to

$$- 2 \frac{(l_t, \epsilon_t(u - k))}{k_t^2} \bar{u}(q + Q) \gamma_{t\mu} \frac{\hat{q}}{q^2} \frac{\hat{k}_t + \hat{l}_t}{\beta_k} \left( 1 + \frac{(2l_t, \epsilon_t(u - k))}{\beta_k \alpha_{ks}} - \frac{\hat{l}_t(\hat{q} - \hat{k}_t)}{\beta_k \alpha_{ks}} \right) v(k - q) \pi. \quad (\text{B.3.9})$$

Further manipulation and the final integration over the azimuth angle of  $l_t$  gives:

$$- \frac{\pi l_t^2}{\beta_k k_t^2} \bar{u}(q + Q) \frac{\hat{q} - \hat{k}_t}{\beta_k \alpha_{ks}} \hat{\epsilon}_t(u - k) v(k - q). \quad (\text{B.3.10})$$

We have to be very careful with  $\alpha_{qs}$ , since it depends on  $k_t$  as well as on  $q$ . From  $(k - q)^2 = 0$  we conclude that

$$\beta_k \alpha_{qs} = (q - k_t)^2. \quad (\text{B.3.11})$$

Next, we consider the diagram in fig. 3.12.b. The value of  $\beta_l$  is now given by the condition  $(q - k + l + u + Q)^2 = 0$ .

$$\beta_l + \beta_u = \beta_k. \quad (\text{B.3.12})$$

For the gluon vertex we have:

$$- 2 (l_t, \epsilon_t(u - k)). \quad (\text{B.3.13})$$

This was already calculated in (B.2.18). We only need the leading order in  $l_t$ , since the second  $l_t$  comes along with the polarization vector of the left t-channel gluon. The propagator

$\frac{1}{(l+u-k)^2}$  just reduces to  $\frac{1}{k_t^2}$ . So we start our calculation with

$$- \frac{(2l_t, \epsilon_t(u-k))}{k_t^2} \bar{u}(q+Q) \hat{p} \frac{\hat{q} - \hat{k} + \hat{l} + \hat{u} + \hat{Q}}{s} \gamma_{t\mu} \frac{\hat{q} - \hat{k} + \hat{l} + \hat{u}}{(q-k+l+u)^2} \frac{\hat{l}_t}{\beta_l + \beta_u} v(k-q) \pi . \quad (\text{B.3.14})$$

For  $(q-k+l+u)^2$  we get  $\beta_k \alpha_q s$ . Further steps lead exactly to the same result as in (B.3.10).

We continue with diagram 3.12.c. The condition that  $(q+l+Q)^2$  equals zero fixes the value of  $\beta_l$ :

$$\beta_l = 0 . \quad (\text{B.3.15})$$

The gluon vertex is the same as in diagram 3.12.a. Instead of expanding the factor  $\frac{1}{\beta_l + \beta_k}$  we now have to expand the propagator  $\frac{1}{(q+l)^2}$ :

$$\frac{1}{(q+l)^2} \approx \left( 1 - \frac{2(l_t, k_t)}{q^2} \right) . \quad (\text{B.3.16})$$

Considering the fermion contribution

$$\frac{2(l_t, \epsilon_t(u-k))}{k_t^2} \bar{u}(q+Q) \hat{p} \frac{\hat{q} + \hat{l} + \hat{Q}}{s} \gamma_{t\mu} \frac{\hat{q} + \hat{l}}{(q+l)^2} \frac{\hat{l}_t + \hat{k}_t}{\beta_l + \beta_k} v(k-q) \pi \quad (\text{B.3.17})$$

we find:

$$\frac{2(l_t, \epsilon_t(u-k))}{k_t^2} \bar{u}(q+Q) \gamma_{t\mu} \frac{\hat{q} + \hat{l}}{(q+l)^2} \frac{\hat{l}_t + \hat{k}_t}{\beta_k} v(k-q) \pi . \quad (\text{B.3.18})$$

Expansion and integration over the azimuth angle of  $l_t$  leads to

$$\frac{\pi l_t^2}{k_t^2 \beta_k q^2} \bar{u}(q+Q) \gamma_{t\mu} \left[ \hat{q} \hat{\epsilon}_t(u-k) + \hat{\epsilon}_t(u-k) \hat{k}_t - \frac{2(q_t, \epsilon_t(u-k))}{q^2} \hat{q} \hat{k}_t \right] v(k-q) . \quad (\text{B.3.19})$$

Finally, we have to investigate the diagram in fig. 3.12.d. Due to the relation  $(q-l-u)^2 = 0$  we get for  $\beta_l$ :

$$\beta_l = -\beta_u + \frac{q^2}{\alpha_q s} . \quad (\text{B.3.20})$$

We do not need to expand in this case, since the numerator is already proportional to  $l_t^2$ . The gluon vertex coincides with that in diagram 3.12.b.

$$\frac{2(l_t, \epsilon_t(u-k))}{k_t^2} \bar{u}(q+Q) \gamma_{t\mu} \frac{\hat{q}}{q^2} \frac{\hat{l}_t}{\beta_l + \beta_u} \frac{\hat{q} - \hat{l} - \hat{u}}{\alpha_q s} v(k-q) \pi . \quad (\text{B.3.21})$$

This is simply evaluated to be

$$\frac{2(l_t, \epsilon_t(u-k))}{k_t^2 \beta_k q^2} \bar{u}(q+Q) \gamma_{t\mu} \frac{\hat{q} \hat{k}_t}{q^2} \hat{q} (\hat{q} - \hat{k}_t) v(k-q) \pi. \quad (\text{B.3.22})$$

which results in the same expression as in eq. (B.3.19).

We now sum up all contributions discussed so far:

$$\begin{aligned} -\frac{2}{\beta_k} \frac{\pi l_t^2}{k_t^2 q^2} \bar{u}(q+Q) \gamma_{t\mu} & \left[ (\hat{q} - \hat{k}_t) \hat{\epsilon}_t(u-k) \frac{q^2}{(q-k_t)^2} + \hat{q} \hat{\epsilon}_t(u-k) + \hat{\epsilon}_t(u-k) \hat{k}_t \right. \\ & \left. - \frac{2(q_t, \epsilon_t(u-k))}{q^2} \hat{q} \hat{k}_t \right] v(k-q). \end{aligned} \quad (\text{B.3.23})$$

We have to remind that with respect to the colour diagram 3.12.a and 3.12.c have opposite sign. The expression above could be brought into the following form:

$$\begin{aligned} -\frac{2}{\beta_k} \frac{\pi l_t^2}{k_t^2 q^2} \bar{u}(q+Q) \gamma_{t\mu} & \left[ 2(q_t, \epsilon_t(u-k)) \left( \frac{(q-k_t)^2}{q^2} + \frac{q^2}{(q-k_t)^2} \right) \right. \\ & - 2(k_t, \epsilon_t(u-k)) \frac{q^2}{(q-k_t)^2} + \frac{2(q_t, \epsilon_t(u-k))}{q^2} \hat{k}_t \beta_k \hat{p} \\ & \left. - \left( 1 + \frac{q^2}{(q-k_t)^2} \right) \hat{\epsilon}_t(u-k) \beta_k \hat{p} \right] v(k-q). \end{aligned} \quad (\text{B.3.24})$$

From now on we have to look at the above expression squared. We leave the factor  $-\frac{2}{\beta_k} \frac{\pi l_t^2}{k_t^2 q^2}$  aside.

$$\begin{aligned} -\frac{2}{q^2} Sp & \left\{ \hat{Q}' \left[ 2(q_t, \epsilon_t(u-k)) \left( \frac{(q-k_t)^2}{q^2} + \frac{q^2}{(q-k_t)^2} \right) - 2(k_t, \epsilon_t(u-k)) \frac{q^2}{(q-k_t)^2} \right. \right. \\ & \left. - \left( 1 + \frac{q^2}{(q-k_t)^2} \right) \hat{\epsilon}_t(u-k) \beta_k \hat{p} + \frac{2(q_t, \epsilon_t(u-k))}{q^2} \hat{k}_t \beta_k \hat{p} \right] \cdot \\ & \cdot (\hat{k} - \hat{q}) \left[ 2(q_t, \epsilon_t(u-k)) \left( \frac{(q-k_t)^2}{q^2} + \frac{q^2}{(q-k_t)^2} \right) - 2(k_t, \epsilon_t(u-k)) \frac{q^2}{(q-k_t)^2} \right. \\ & \left. \left. - \left( 1 + \frac{q^2}{(q-k_t)^2} \right) \beta_k \hat{p} \hat{\epsilon}_t(u-k) + \frac{2(q_t, \epsilon_t(u-k))}{q^2} \beta_k \hat{p} \hat{k}_t \right] \right\}. \end{aligned} \quad (\text{B.3.25})$$

The trace is easily evaluated, but the reduction afterwards is quite lengthy. We frequently make use of the following equations:

$$\begin{aligned} (q_t - k_t)^2 &= (1-z)(q-k_t)^2; \\ q^2 - q_t^2 &= z(q-k_t)^2. \end{aligned} \quad (\text{B.3.26})$$

where we define  $z$  as  $\frac{\beta_q}{\beta_k}$ . Expression (B.3.25) then transforms into

$$\begin{aligned}
& -\frac{8\beta_k s}{q^2} \left\{ (1 - 2z + 2z^2) \frac{q^2}{(q - k_t)^2} - 4 \frac{k_t^2 q_t^2 - (k_t, q_t)^2}{q^2 (q - k_t)^2} \right. \\
& \quad + 2(1 - z) + (1 - 2z + 4z^2) \frac{(q - k_t)^2}{q^2} \\
& \quad \left. - 2z \frac{(q - k_t)^4}{q^4} + 2z^2 \frac{(q - k_t)^6}{q^6} \right\} . \tag{B.3.27}
\end{aligned}$$

Since we are interested in the higher twist contribution  $\frac{1}{q^4}$ , we will expand the above expression with respect to the smallness  $\frac{k_t^2}{(1-z)q^2}$ . In order to do this we first have to express  $\frac{(q - k_t)^2}{q^2}$  in terms of  $|k_t|$ ,  $|q|$  and the azimuth angle  $\varphi$ :

$$\frac{(q - k_t)^2}{q^2} \approx 1 - 2\sqrt{1 - z} \frac{|k_t|}{|q|} \cos \varphi + \frac{|k_t|^2}{|q|^2} (1 - 2z \cos^2 \varphi) . \tag{B.3.28}$$

This expression introduced in (B.3.27) leads to the final answer

$$-\frac{32\beta_k s}{q^2} \left\{ 1 - 2z + 2z^2 + 3z(1 - z)(2z - 1) \frac{l_t^2}{q^2} \right\} . \tag{B.3.29}$$

The first term in curly brackets is the standard Altarelli-Parisi splitting function. The result that we were looking for is the next to leading contribution, i.e. the second term in curly brackets.

In fig. 3.14 we present one example of a set of diagrams which do not contribute. The reason is simple. The diagram 3.14 gives instead of one factor  $\frac{1}{\beta_k}$  the less singular  $\frac{1}{\beta_u}$ . After squaring, the result will be proportional to  $\frac{x}{\beta_u} \ln\left(\frac{x}{\beta_u}\right)$  whereas the leading contributions corresponding to diagram 3.12 are of the order of 1.

To conclude this subsection we have to add the colour coefficient which corresponds to expression (B.3.29). All our calculations were normalized to diagram 3.12. Looking at this diagram squared (fig.3.15) we get

$$\frac{1}{8} \frac{N^2}{N^2 - 1} . \tag{B.3.30}$$

## References

- [1] A.H. Mueller, J. Qui: Nucl. Phys. B268, 427 (1986).

- [2] A.B. Kaidalov, K.A. Ter-Martirosyan: Nucl. Phys. B75, 471 (1974).
- [3] V.A. Abramovskii, R.G. Betman: Sov. J. Nucl. Phys. 49, 1205 (1989).
- [4] L. V. Gribov, E. M. Levin and M. G. Ryskin: Phys.Rep. C 100, 1 (1983) .
- [5] J. Bartels, G. Ingelman: Phys. Lett. B235, 175 (1990).
- [6] M.G. Ryskin: Sov. J. Nucl. Phys. 52, 529 (1990).
- [7] N.N. Nikolaev, B.G. Zakharov: preprint DFTT-5/91, Z. Phys. C49, 607 (1991), Phys. Lett. B260, 414 (1991).
- [8] G. Ingelman, P.E Schlein: Phys. Lett. 152B, 256 (1985).
- [9] L. Frankfurt, M. Strikman: Phys. Rev. Lett. 63, 1914 (1989)
- [10] A. Donnachie, P.V. Landshoff: Nucl. Phys. B244, 322 (1984).
- [11] E.L. Berger et al.: Nucl. Phys. B286, 704 (1987).
- [12] G. Ingelman, K. Janson-Prytz: Phys. Lett. B281, 325 (1992).
- [13] V.A.Abramovski, V.N. Gribov and O.V. Kancheli: Sov.J.Nucl.Phys 18, 308 (1973).
- [14] V.V. Sudakov, ZhETF 30, 187 (1956).
- [15] V.N.Gribov,L.N.Lipatov : Sov. J. Nucl. Phys. 15 ,438 (1972)  
L.N.Lipatov : Yad. Fiz. 20, 181, (1974)  
Yu.L. Dokshitzer: Sov. Phys. JETP 46, 641 (1977)  
G. Altarelli, G. Parisi: Nucl. Phys. B126, 298 (1977).
- [16] A. Bassetto, M. Ciafaloni, G. Marchesini: Phys. Rep. 100, No. 4, 201 (1983)
- [17] J. Bartels, E.M. Levin: preprint DESY 92-033 (1992).
- [18] J.Bartels: preprint DESY 92-114 (1992).
- [19] E.M. Levin, M.G. Ryskin, A.G. Shuvaev: preprint DESY 92-047 (1992), Nucl. Phys. B ( in print ).
- [20] A. Capella, A. Krzywicki, E.M. Levin: Phys. Rev. D44, 704 (1991).
- [21] Yu. L. Dokshitzer, D. I. Dyakonov and S. I. Troyan: Phys. Rep. 58, 269 (1980).
- [22] M. Wüsthoff: Diplomarbeit, unpublished.

## Figure Captions:

- fig. 1.1:* Relation between the diffractive dissociation and triple Pomeron diagram.
- fig. 1.2:* Diffractive dissociation with Pomeron exchange.
- fig. 2.1:* The Pomeron as QCD-ladder.
- fig. 2.2:* The QCD-model of the diffractive dissociation in the Triple Regge Limit.
- fig. 2.3:* Graphical representation of the Pomeron proton interaction described by the amplitude  $M$ .
- fig. 2.4:* Screening (shadowing) correction to the proton structure function.
- fig. 2.5:* Additional gluon production leading to logarithmic contribution below the cell with  $\frac{dk^2}{k^4}$ -integration.
- fig. 3.1:* Complete set of diagrams which contribute to the two quark production at Born level.
- fig. 3.2:* u-channel contribution corresponding to the diagrams in *fig. 3.1*.
- fig. 3.3:* We use these diagrams to explain the Ward identity in the t-channel.
- fig. 3.4:* Graphical representation of the colour singlet projector.
- fig. 3.5:* The colour contents of this diagram leads to the factor  $C_F$ .
- fig. 3.6:* The squared amplitude of two quark production (Born level).
- fig. 3.7:* The first set of diagrams for the three jet production (two quarks and one gluon).
- fig. 3.8:* The second set of diagrams for the three jet production.
- fig. 3.9:* One example of diagrams which does not contribute in the leading log approximation. The diagram is the same as in *fig 3.8.c*, but the kinematic is different.

*fig. 3.10:* Colour coefficient of the three jet production.

*fig. 3.11:* The squared amplitude of the three jet production. The gluon jet in a) has a distribution  $\frac{dk_t^2}{k_t^4}$  whereas in b) it has the log distribution  $\frac{dq_t^2}{q_t^2}$ .

*fig. 3.12:* Three jet production which corresponds to the higher twist contribution  $\frac{dq^2}{q^4}$ . The circle which is drawn for the triple gluon vertex indicates the necessity to use the effective vertex which consists of the sum of the three diagrams in fig. 3.13.

*fig. 3.13:* Contributions to the effective vertex in fig. 3.12.

*fig. 3.14:* Noncontributing diagram.

*fig. 3.15:* Colour structure which corresponds to the square of the diagrams in fig. 3.7 and 3.8.

*fig. 4.1:* Generalization to any number of jet emission.

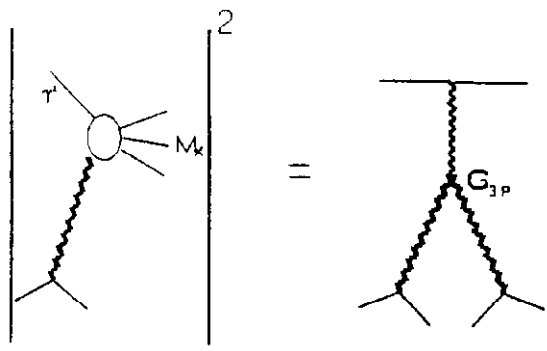


fig. 1.1

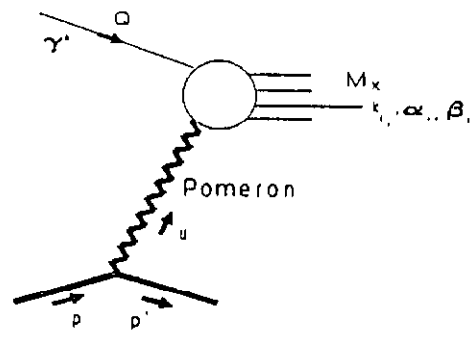


fig. 1.2

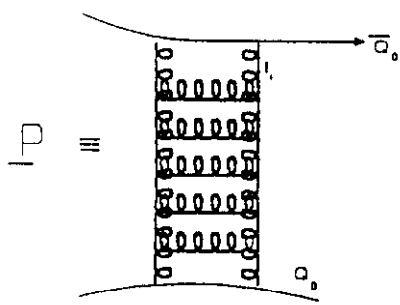


fig. 2.1

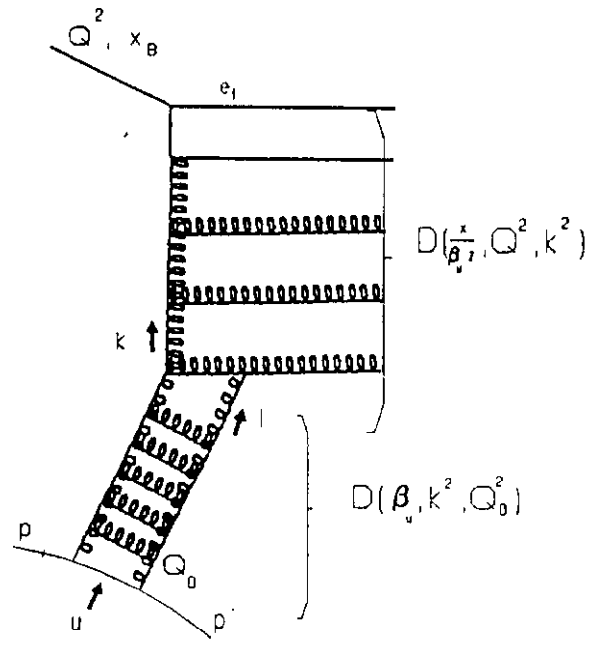


fig. 2.2

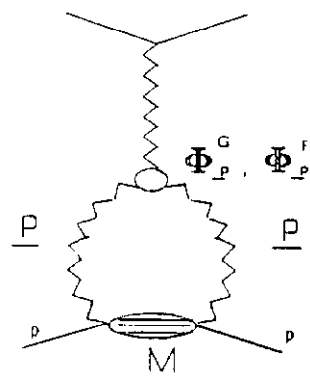


fig. 2.3

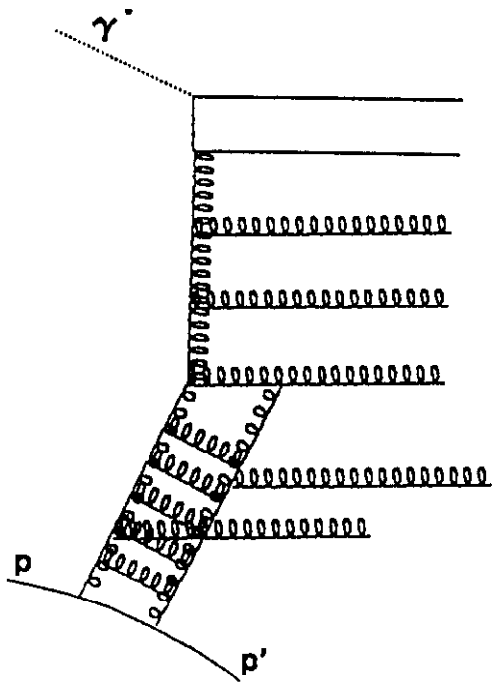


fig. 2.4

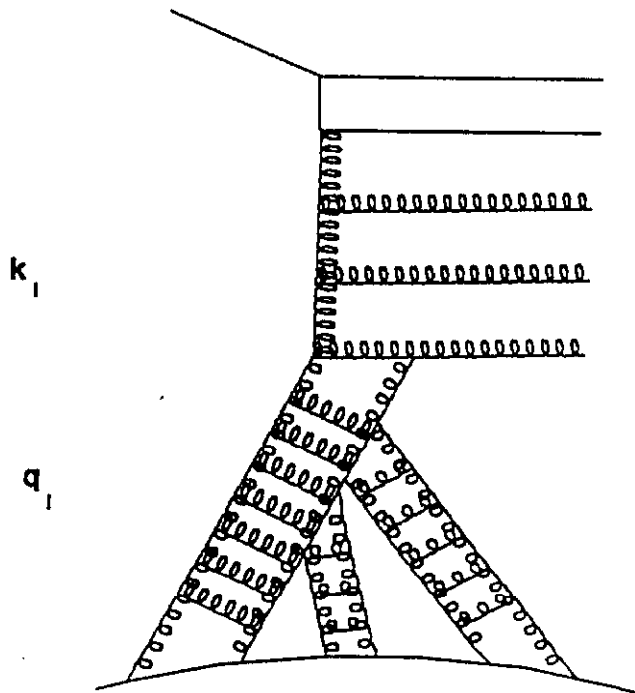


fig. 2.5

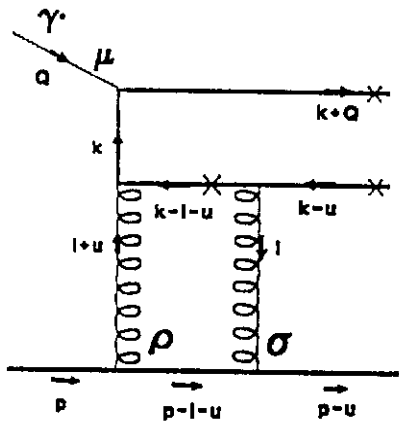


fig. 3.1.a

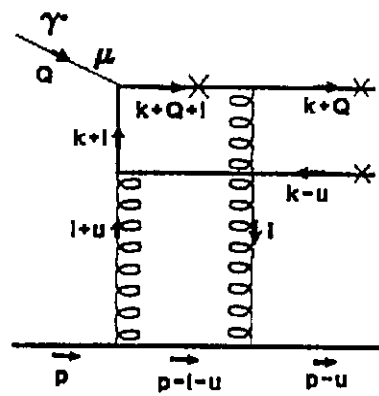


fig. 3.1.b

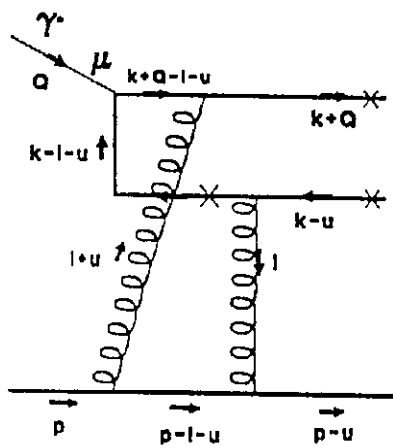


fig. 3.1.c

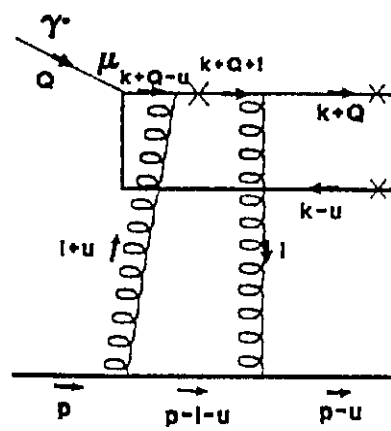


fig. 3.1.d

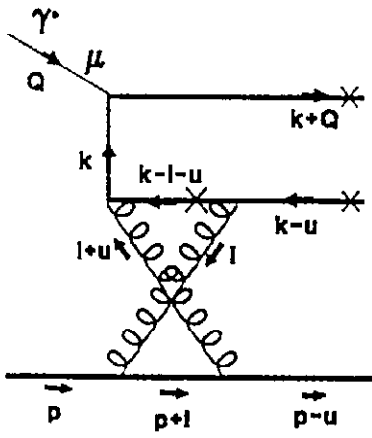


fig. 3.2

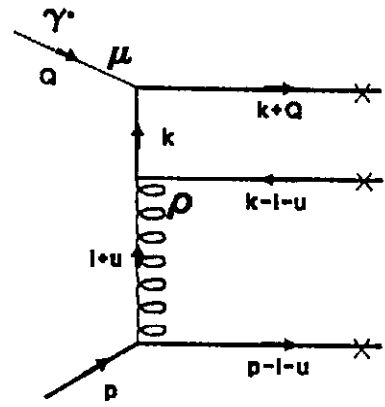


fig. 3.3.a

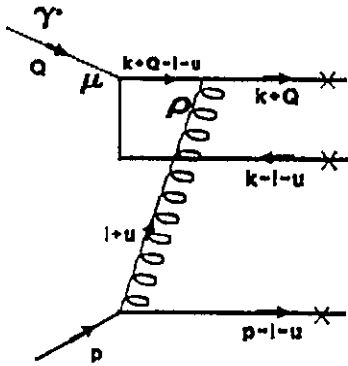


fig. 3.3.b

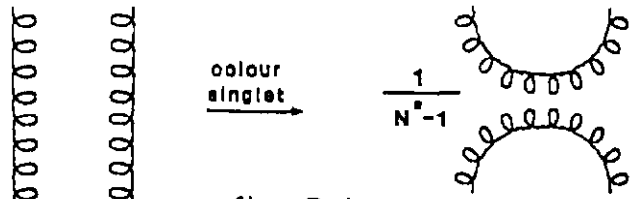


fig. 3.4

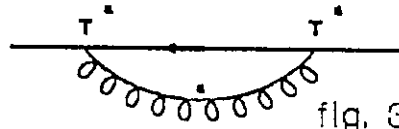


fig. 3.5

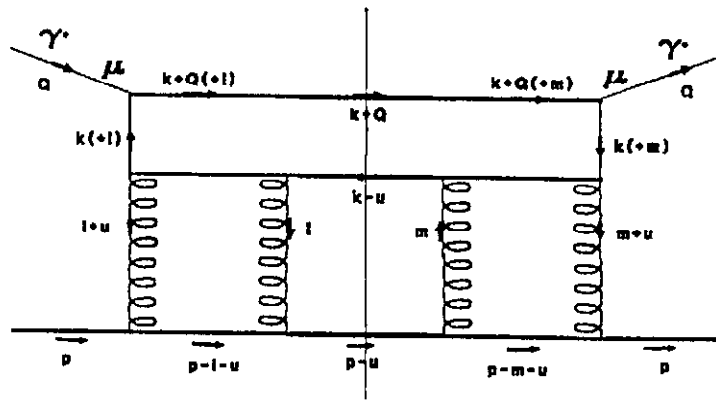


fig. 3.6

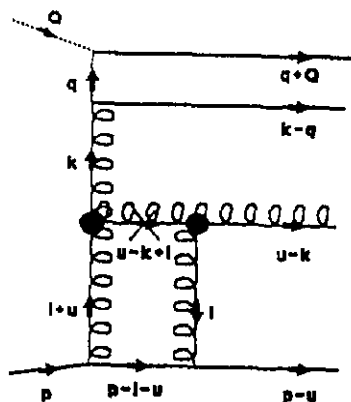


fig. 3.7.a

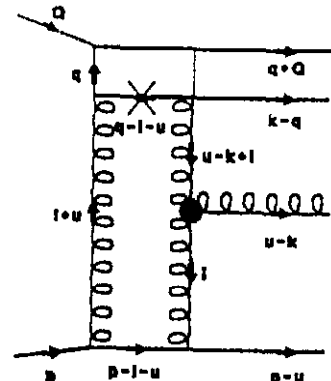


fig. 3.7.b

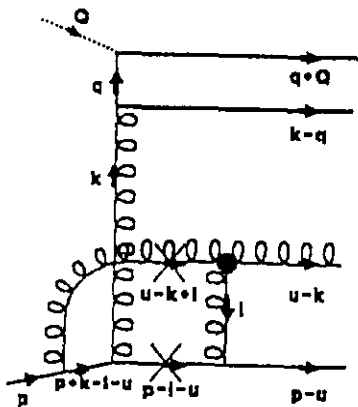


fig. 3.7.c

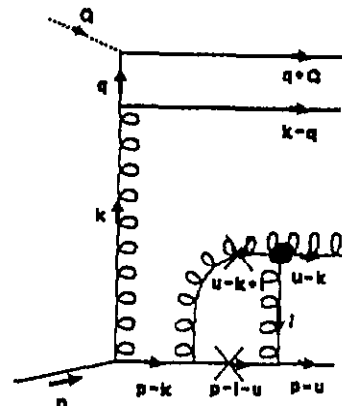


fig. 3.7.d

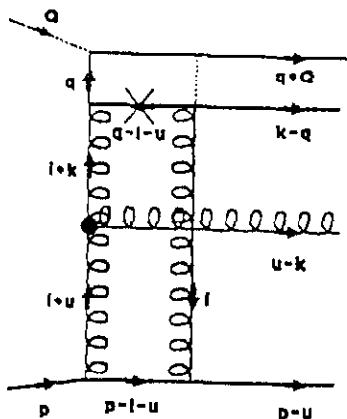


fig. 3.8.a

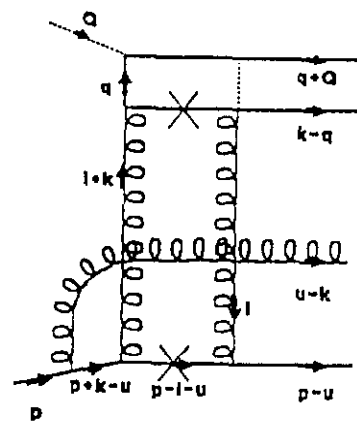


fig. 3.8.b

fig. 3.11.a

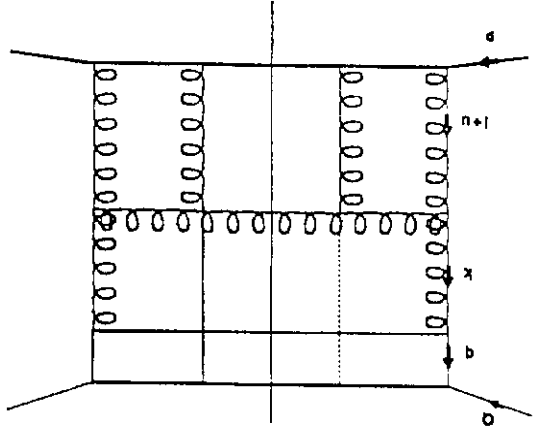


fig. 3.11.b

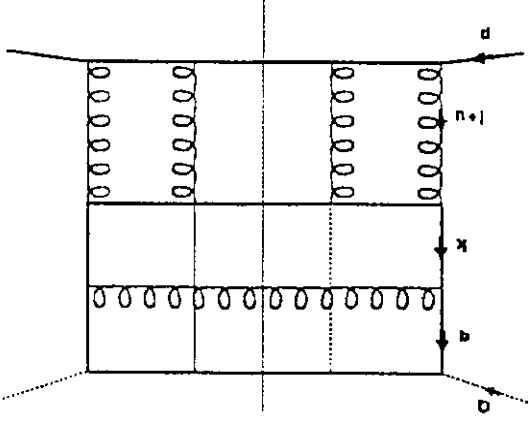


fig. 3.10

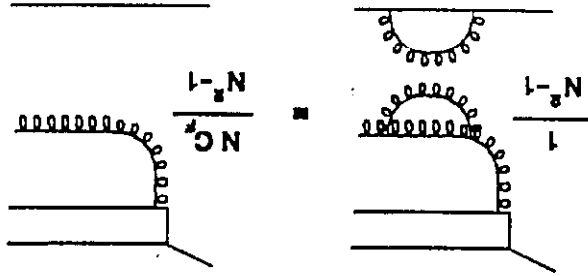


fig. 3.8.c

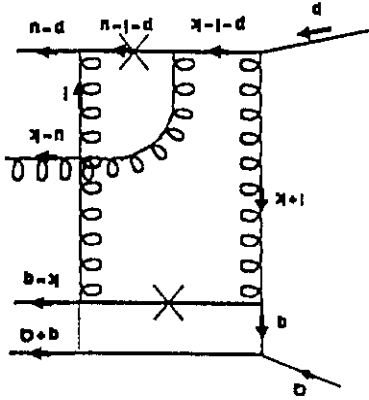
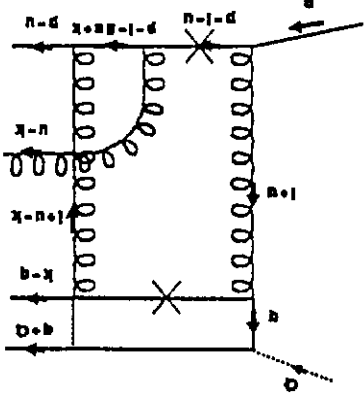


fig. 3.9



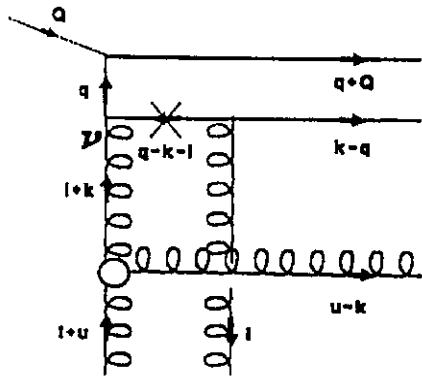


fig. 3.12.a

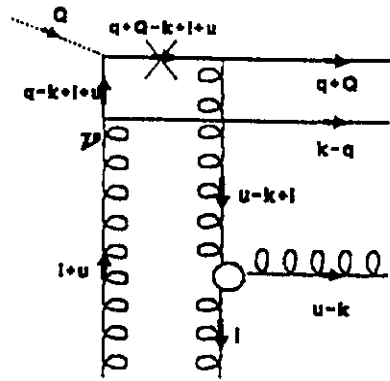


fig. 3.12.b

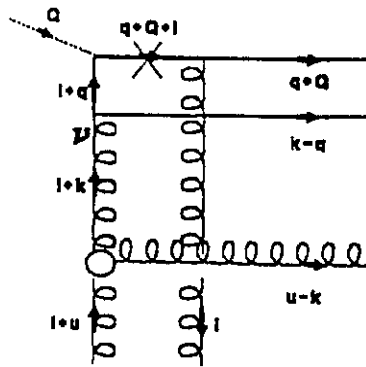


fig. 3.12.c

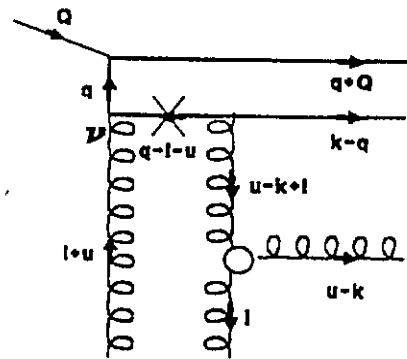


fig. 3.12.d

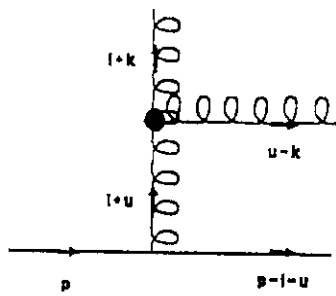


fig. 3.13.a

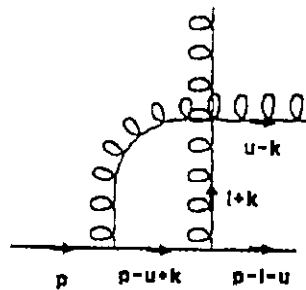


fig. 3.13.b

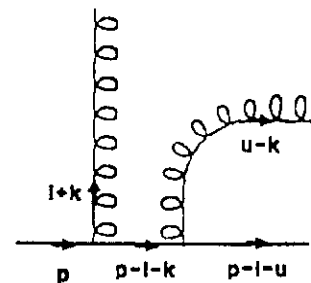


fig. 3.13.c

fig. 4.1

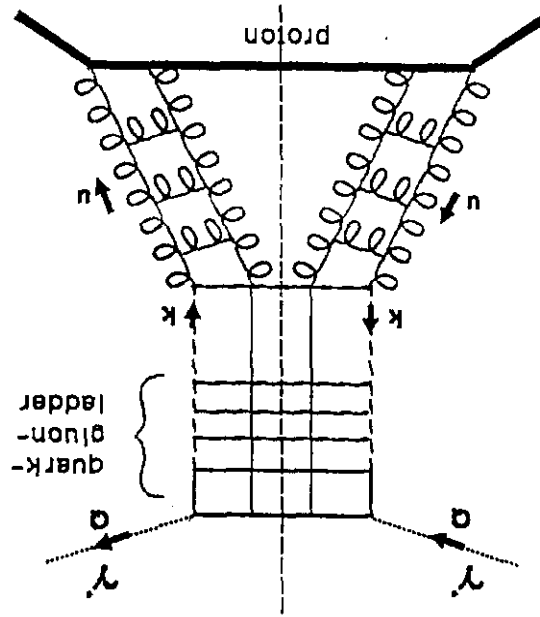


fig. 3.15

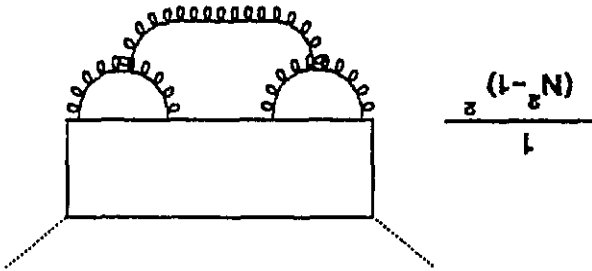


fig. 3.14

